

Fatigue of Wood
as related to
Defects and Creep

by

Lauge Fuglsang Nielsen

Building Materials Laboratory
Technical University of Denmark
Building 118
DK-2800 Lyngby, Denmark



THE TECHNICAL UNIVERSITY OF DENMARK
DEPARTMENT OF CIVIL ENGINEERING
BUILDING MATERIALS LABORATORY

Fatigue of Wood as related to Defects and Creep

by

Lauge Fuglsang Nielsen

SUMMARY

A lifetime theory has previously been developed by the present author which considers wood subjected to ramp- and deadload mainly.

The theory (DVM-theory) which is based on the concept of wood behaving as a Damaged Viscoelastic Material has been shown to describe successfully the lifetime behavior of both clear wood and structural wood. Also other aspects of wood behavior like tertiary creep and stiffness-strength relations, strength reduction due to sustained load and lifetime dependency on wood quality can be explained by the theory.

The present article expands the DVM-theory such that cyclic loading is also considered. This means that fatigue lifetime solutions are established which relate defect structure, viscoelasticity, load amplitude, fractional time under maximum load, and load frequency. The conventional (elastic) fatigue phenomenon is hereby approached at high frequency loading. Also deadload lifetime is included as a special case.

The analysis includes prediction of residual quantities of strength and critical stress intensity factor during the process of fatigue. The effects of a possible load threshold below which no fatigue occurs is discussed in the final section of the article.

KEYWORDS

Wood, Fatigue, Cyclic load, Fracture Mechanics, Viscoelasticity, Creep, Relaxation

Contents

Chap 1:	INTRODUCTION	Page 1
1.1	Basics of analysis	2
Chap 2:	FAILURE OF WOOD	7
2.1	Crack model and strength level	10
2.1.1	Basic wood	11
2.1.2	Clear wood	11
2.1.3	Structural wood	12
Chap 3:	RHEOLOGY OF WOOD	16
3.1	Relaxation time and creep power	17
3.2	Local relaxation time at failure	18
3.2.1	Clear wood	19
3.2.2	Structural wood	20
Chap 4:	FATIGUE ANALYSIS	22
4.1	Elastic crack closure relations	24
4.2	Elastic-viscoelastic counterparts	26
4.2.1	Time shifted creep function	26
4.2.2	Viscoel. amplitude amplification	29
4.3	Damage rate	30
Chap 5:	GENERALIZATIONS	34
5.1	Multi-damage systems	34
5.2	Arbitrary load ratio	35
Chap 6:	APPLICATION OF FATIGUE THEORY	36
6.1	Numerical basis	37
6.2	Experiments and theory	40
6.3	Fatigue predictions	45
6.3.1	Residual strength	46
6.3.2	Residual K_{cr}	46
6.3.3	Lifetime-frequency relation	47
6.3.4	Estimates and lifetime presentation	50
6.3.5	Threshold	52
Chap 7:	CONCLUSIONS AND FINAL REMARKS	54
7.1	Final remarks	55
Acknowledgments		56
Literature		57
Appendices		60
A:	On orthotropic crack analysis	60
B:	On Viscoelastic crack closure	69
C:	Numerical lifetime analysis	82

Chapter 1

Introduction

Fatigue in engineering material is defined as the progressive damage and failure that occurs when the material is subjected to repeated loads of a magnitude smaller than the static strength.

Fatigue reduces the materials strength and lifetime to a degree which has to be considered in design of structures. Frequency of loading is here an important parameter. This is clearly demonstrated by the results presented by Bach (1) from tests on clear wood subjected to compressive cyclic loading with a minimum load of 0. At a maximum load of about 75 % of short time strength lifetime number of cycles decreased by a factor 1000 lowering the frequency from 1 per 10 seconds to 1 per day.

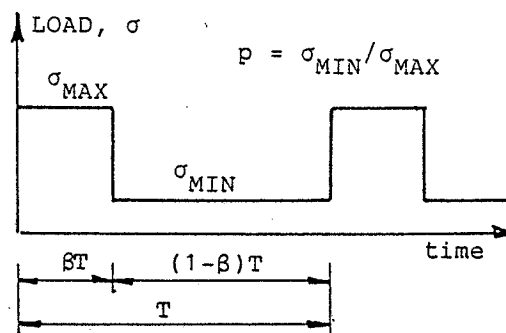


Figure 1.1 Square wave loading considered in the fatigue analysis. Load ratio is defined by $p = \sigma_{MIN} / \sigma_{MAX}$. Wave period is T and fractional time under maximum load is β .

These introductory comments define the topic of the present article:

Relations are developed which predict lifetime and remaining strength of clear wood and structural wood subjected to varying loads. The possibility of a threshold

on load below which no fatigue occurs is discussed in the final section of the article.

The load history considered is outlined in Figure 1.1. Maximum load and minimum load are denoted by σ_{MAX} and σ_{MIN} respectively. Load ratio is defined by $p = \sigma_{\text{MIN}}/\sigma_{\text{MAX}}$. Wave period is T and fractional time under maximum load is β .

1.1 BASICS OF ANALYSIS

Two basic observations on the structure and mechanical behavior of wood are maintained in the present analysis: 1) Wood has a natural content of defects and defect nuclei (like knots and inherent cracks), and 2) Wood exhibits time dependent behavior (creep).

It is logical to state the hypothesis that wood behaves like a Damaged Viscoelastic Material (2). On this basis a lifetime theory (referred to as the DVM-theory) has previously been developed by the present author which considers wood subjected to ramp- and deadload mainly (e.g. 3,4).

The DVM-theory has been shown to describe successfully the lifetime behavior of both clear wood (5,6) and structural wood (7,8,9). Also other aspects of wood behavior like tertiary creep and stiffness-strength relations, strength reduction due to sustained load and lifetime dependency of wood quality (10,11,4,12) can be explained by the theory.

It seems hereby justified that the concept of wood behaving as a damaged viscoelastic material is a realistic basis of developing further the DVM-theory such that also fatigue lifetime can be considered.

The basic damage model used is the so-called Dugdale model (13) shown in Figure 1.2. The coherent stress, σ_1 , at the crack front may be thought of as being the materials theoretical strength. (Material pulled out into the crack front zone is hereby considered to be stiff and perfectly plastic).

As shown in Figure 1.2 the Dugdale model represents a so-called mode I (or opening mode) crack in an isotro-

pic material. This is incidentally. The model applies as well for cracks in mode II (sliding, shear in the xy-plane) and mode III (tearing, shear in the xz-plane). Load and coherent stress indicated in Figure 1.2 should then be interpreted as appropriate shear load and shear strength quantities respectively. Apart from this the results of an analysis based on the opening mode version of the Dugdale model only differ by the elastic coefficients from results applying for other modes. In a similar way the Dugdale model also applies for orthotropic materials like wood. Here however, it is required that crack planes coincide (as they actually do in wood) with the principal planes. (The changes of elastic moduli according to mode - including the orthotropic case - are given in Appendix A at the end of the article).

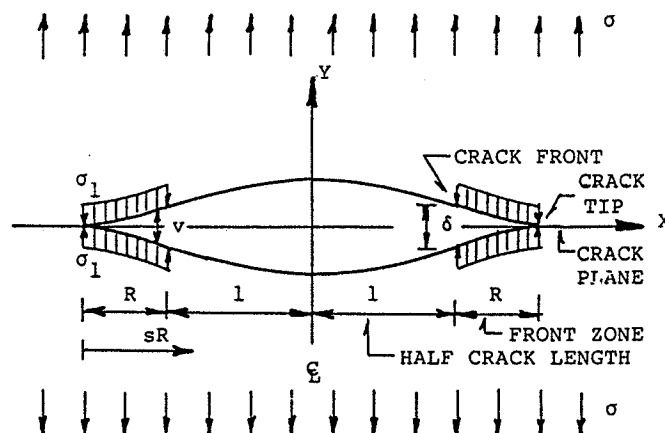


Figure 1.2. Dugdale model. Terminology used in the present paper. Load is denoted by σ , coherent stress by σ_1 .

The consequences of the above considerations are that it is possible (3) to generalize a lifetime analysis based on the isotropic, opening mode results only by normalizing with respect to the short time results (time Θ^+). In this way, mode and other features defining the crack problem like stress situation (e.g. plane stress, plane strain) type of coherent stress, orthotropy, and failure criterion for example are considered in total by the materials respective short time strength.

One restriction, however, apply to this normalizing procedure. An assumption of balanced creep has implicitly been applied. Balanced creep means that time dependency of fractional creep is independent of direction. Previous lifetime studies by the present author (3 f.ex) have been based on an appropriately estimated average creep behavior of wood. In the present study a theoretically more correct conception of orthotropic creep is included.

"Dimensionless lifetime analysis" referred to in the subsequent text is synonymous with "normalized lifetime analysis" as defined by these comments.

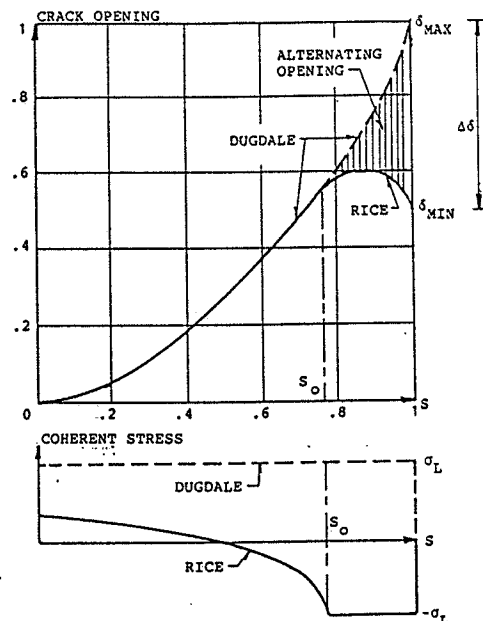


Figure 1.3. Results of the Rice crack closure model. Referring to the load history shown in Figure 1.1 δ_{MAX} and δ_{MIN} mean crack front opening at $\sigma = \sigma_{MAX}$ and σ_{MIN} respectively. $\Delta\delta$ is the alternating front opening.

A lifetime analysis of cracked viscoelastic materials subjected to non-decreasing loads is relatively simple to establish using the Dugdale model. This has been shown in (3) for example.

For decreasing loads, however, some modifications (not disturbing the normalizing features just described) have to be introduced which consider the phenomenon of

crack closure: The opening of a crack is not a reversible process. Material which has been pulled out into the crack front when defects are opened under increasing load will oppose closure at decreasing load. The influence of crack closure on the elastic fatigue lifetime of wood has been studied by the present author in (14) on the basis of the Rice-modified Dugdale model (15) some results of which are outlined in Figure 1.3. The inclusion of the crack closure phenomenon in the DVM-theory forms the central point of the present analysis such that viscoelastic fatigue lifetime can also be predicted.

For this purpose some considerations on viscoelastic crack closure are presented in Appendix B at the end of the paper. Readers, however, interested especially in modifying the Dugdale model (and its Rice modification) for application to elastic fatigue of wood are referred to (14). No full explanation of this topic will be given in the present paper. Only final results relevant for the analysis of viscoelastic fatigue will be presented here).

It should be emphasized that the results obtained in the following are not bound to a defect system which literally consists of cracks. Dislocations, for example, may also be the defect source. It is well known that the effects of a climbing group of edge dislocations are described exactly by the same equations which govern the crack problem. At vital points of the analysis we therefore introduce the dimensionless quantities, "damage" (in stead of crack length) and "damage rate" (in stead of crack velocity). In this way the analysis takes the form of a so-called theory of damage accumulation.

Being the very basics of the analysis presented damage and creep of wood are topics which have to be considered rather detailed prior to the real analysis.

Section 2 below presents the authors opinion on how we may model the overall failure mechanism of wood. Basically the first part of the section is a summary of

some thoughts which were made in (14) in the context of an elastic fatigue analysis of wood.

The rheology of wood is considered in Section 3.

Chapter 2

Failure of Wood

Wood is a material which is orthotropic in such a way that cracks can only propagate parallel to grain. This means that any attempt of a crack to cross grain (outside weak areas) is blunted by branching off parallel to grain. (We exclude here very high speed, impact loading).

Clear wood may be thought of as a "multiple finger joint material". The ratio of finger length, L , to finger root diameter, d , is of magnitude, $L/d \approx 8$.

A finger may be considered as the end of a "super fiber" made by bundles of wood fibers. (The extreme case of a super fiber being a single wood fiber is not excluded).

The boundary between fingers is produced by crack extension parallel to grain. The cracks involved in this process originate primarily from the many inherent defect nuclei like bad bonding between tracheids, ineffective overlapping zones, pit concentrations and rays. Handling of wood, drying for example, creates internal stresses at natural inhomogeneities by which some of the defect nuclei - including those with a perpendicular to grain direction - turn into cracks with a leading edge parallel to grain, see Figure 2.1. An average slope of $d/(2L) \approx 1/16$ of the final failure surface (relative to grain) is made possible by a characteristic rhythm of the defect nucleus structure (size, distance, orientation, and distribution).

The cracks expand parallel to grain in a combined sliding and opening mode. The path of expansion is indicated by the pattern of defect nuclei and neighbouring cracks. At perpendicular to grain loading the opening mode is the overriding mode producing in the end a cleavage surface by coalesce of nearly co-linear cracks. At parallel to grain loading both modes are active with sliding as the dominant part. Again failure occurs by coalesce of nearly colinear cracks producing

the typical "finger splintering" type of failure surface.

A "cross grain" failure is no exception in this respect. The fingers, however, may be small, leaving - for the naked eye - an apparently smooth failure surface.

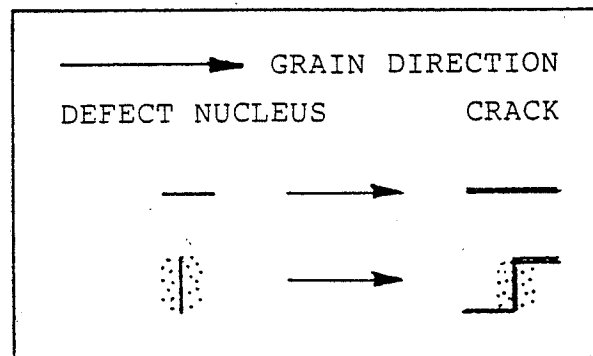


Figure 2.1. Basic elements of a failure model for wood. Dots indicate weak area. Reproduced from (14).

The same crack system is activated for both perpendicular and parallel to grain tensile loading. Only mode of failure and stress state change. As we shall base our fatigue analysis on dimensionless quantities we can then in principles apply the solutions obtained irrespective of load direction. This has been shown in (14): All basic information on the materials elastic behavior, failure mode and stress state needed for a failure analysis are considered in total by the short time strength defining the so-called load level, $SL = \text{load/strength}$. (Simple modifications considering orthotropic creep will be introduced in a subsequent section).

A special consequence of the failure model suggested is that perpendicular to grain and parallel to grain tensile strength (and shear strength along the grain) for clear wood are equally damage influenced, meaning that their ratios remain a constant.

At compression parallel to grain where the load is low enough not to induce instability of the fibers (or the super fibers previously defined) the "tensile" mechanism described above is still a possible fatigue failure mechanism. At higher compressive loads the mechanism acts as an introductory mechanism. At a certain stage, however, two additional failure mechanisms become activated: 1) A "finger joint wedge" mechanism bringing the finger roots into an opening mode tensile state, and 2) A mechanism of instability: The fibers are "cut free" to a length which is not stable - and a failure band of crushed, overturned fibers will show up perpendicular to grain.

In principle the failure mechanisms of structural wood and clear wood are similar. However, an overriding system of major defects like knots and handling defects are now the stress concentrators responsible for failure. Handling of structural wood, drying for example, creates internal stresses at these inhomogeneities by which major cracks are developed. Due to the special orthotropic strength distribution in wood these cracks - including those having a "thickness", i.e. a perpendicular to grain origin - will orientate themselves parallel to grain; attempts to cross grain away from defect nuclei and minor defects are blunted. In principle Figure 2.1 also illustrates the formation of major cracks. The size of a major crack and a characteristic dimension of its nucleus will have the same order of magnitude.

Two principal failure types of axially loaded structural wood may develop from major cracks.

Local failure: Major defects are involved in this failure type mainly by separating the area considered into an ineffective part, shadowed by the defect thickness, and an effective part where clear wood failure proceeds as previously described.

Non-local failure: Major cracks are actively involved in the fracture process, meaning that they are part of a nearly colinear crack system producing a far reaching finger joint failure surface. Major defects propagate along paths also preferred by minor cracks.

Practically structural wood failure is a composite of local and non-local failure. The "winning" type is the one producing the lower load capacity.

At compression the wedge and instability effects previously considered are of importance primarily for clear wood and structural wood with local failure. When structural wood is considered with non-local failure involving large and far reaching fingers indicated by knots (and other larger defects) sliding as considered in the tensile situation of clear wood will be the overriding mechanism. Areas of crushing will be local and relatively small. A special consequence of this statement is that structural wood may have tensile and compressive strengths which are not too different.

The overall failure model suggested in this section is invariable with respect to crack distance. However, an assumption of widely separated (non-interacting) major defects may be introduced. This assumption is supported by the fact that deadload and rampload lifetime predictions based on a single-crack model are shown to explain successfully a number of experimental data (5,6,7,8,11).

Accepting (as we do in this paper) the above failure hypothesis only minor modifications have to be introduced in the subsequent fatigue analysis going from tension to compression parallel to grain. The crushing phenomenon in compression is considered approximately reducing the failure resistance proportional to strength. This means $K_{cr}(\text{compression}) \approx 0.5 * K_{cr}(\text{tension})$.

2.1 CRACK MODEL AND STRENGTH LEVELS

The above considerations will now be summarized and quantified from a simple composite and crack mechanical point of view: Structural wood is clear wood damaged by a single major defect. Clear wood is basic wood damaged by minor defects.

It has been indicated in Section 2 that a single-damage model applies practically well in lifetime studies of

deadloaded structural wood. It is anticipated that this feature also applies when the fatigue phenomenon is studied. However, not to exclude exceptions an easy method is given in Section 5 which generalize the results obtained also to apply when interacting major defects are present.

2.1.1 BASIC WOOD

Basic wood is the plain, nature given wood material without any of the numerous defect nuclei having been developed into cracks. The strength, σ_1 , and critical stress intensity factor, K_{Ic} , can be related approximately as follows

$$\sigma_1 \approx \frac{K_{Ic}}{\sqrt{\pi a}} \quad (2.1)$$

where a is a characteristic dimension of a defect nucleus. Equation 2.1 represents the approximate upper strength bound for which the well-known Griffith strength expression applies: $\sigma_{Ic} = K_{Ic}/\sqrt{\pi l}$ where strength and crack half-length are denoted by σ_{Ic} and l respectively).

It is not possible from existing experimental literature to quantify size and density (number/unit area) of defect nuclei. Plausible order of magnitudes, however, might be the following as estimated by the present author on the basis of micro structural photographs: The nucleus "radius" is $a \approx 0.15$ mm. The density is $\approx 5/\text{mm}^2$ corresponding to 1 nucleus per fiber along the grain and 1 per 5 fibers perpendicular to grain.

2.1.2 CLEAR WOOD

This material is basic wood where some of the defect nuclei have transformed into minor cracks. We model the strength behavior of clear wood by a parallel to grain array of equally sized cracks of length, $2l_o$, and a center distance, $2b$. (Index o on l indicate initial size of minor crack)

The strength of a material such weakened is given by the Griffith expression modified to include interaction effects,

$$\sigma_{cr} \approx \frac{K_{Gr}}{\sqrt{(\pi l)}} \frac{1}{f_w(l_w/b)} \quad (2.2)$$

where the interaction factor, $f_w = f(l_w/b)$, is given by the following simple expression suggested in (10),

$$f_w \approx [1 - (l_w/b)^2]^{-1/2} \quad (2.3)$$

Introducing Equation 2.1 Equation 2.2 can also be written,

$$FL = \frac{\sigma_{cr}}{\sigma_1} \approx f_w^{-1} \sqrt{a/l_w} \quad (2.4)$$

which defines the so-called strength level, FL. Respecting that $\sigma_{cr} \leq \sigma_1$ we have $FL \leq 1$ at $l_w < a$. A graphical representation of Equation 2.4 is given in Figure 2.2.

Schniewind & Lyon (16) suggested that normal clear wood contains inherent cracks of size $2 \times l_w \approx 2.5$ mm. (We will use $l = 1.5$ mm). If we assume that these cracks are widely distributed ($l_w/b < 1/3$) Equation 2.6 predicts a strength level of $FL \approx 1/3$ for clear wood. Of course, this value is not invariable. Bad drying, for example, may have produced larger defects such that $FL < 1/3$ is predicted.

At more closely situated minor cracks the strength level will decrease. For example, when $l_w/b = 0.6$ is introduced we get $f_w = 1.25$ and $FL \approx 1/4$.

As is the case for defect nuclei we cannot from existing literature quantify distance between minor cracks. A reasonable guess might be that every second nucleus develop into a minor crack. This means $b \approx 3$ mm corresponding to $a/b \approx 1/20$ (and $l_w/b \approx 0.5$).

2.1.3 STRUCTURAL WOOD

Structural wood is clear wood containing major defects like knots and cross sawing. Following the failure model suggested in Section 2 where failure is in general a result of damage propagation parallel to the

grain we expect that the major defects in structural wood become responsible (by drying or loading) for amplification of minor defects parallel to grain. The local amplification is such that cracks of a size equal to the major defects turn up. A knot, for example, is responsible for a parallel to grain crack length, $2L \approx D$, where D is knot diameter.

Local failure: As indicated in Section 2 local failure in axially loaded structural wood is the result of clear wood failure in an area reduced proportional to the perpendicular to grain dimension of the major defect considered.

Non-local failure: Also indicated in Section 2 is a failure type where the major cracks are included directly in the strength reducing crack system applying for clear wood. In this case strength of structural wood may be predicted approximately by means of the composite critical stress intensity factor, K^* , given in Equation 2.6 below. For a single major defect we get

$$\sigma_{cr} \approx \frac{K_{cr}^*}{\sqrt{(\pi L)}} = f^{-1} * \sqrt{a/L} \quad (2.5)$$

where L is (half) length of the major defect.

The composite critical stress intensity factor, K^* , used above is given by

$$\frac{K_{cr}^*}{K_{cr}} \approx f_0^{-1} \quad ; (K_{cr} = \sigma_1 \sqrt{\pi a}) \quad (2.6)$$

obtained by Equation 2.2 considering approximately the uniform crack array solution as the result of placing a single crack in a matrix weakened by cracks of the same kind.

The composite coherent stress, σ_1^* , at a crack front can be approximated by Equation 2.6 as follows when the well-known relation, $K_{cr} = \sqrt{(E\sigma_1\delta_{cr})}$, is introduced relating stress intensity factor to Young's modulus, E , coherent stress, σ_1 , and critical crack front opening, δ_{cr} (= critical crack opening displacement, COD). We get

$$\frac{E\sigma_1^*\delta_{cr}^*}{E\sigma_1\delta_{cr}} \approx f_0^{-2}$$

still with * indicating composite property. This expression gives us the composite coherent stress as follows when we anticipate that stiffness and critical COD only change slightly compared with the variation of σ_1^* .

$$\frac{\sigma_1^*}{\sigma_1} \approx f_0^{-2} \quad (2.7)$$

It should be noticed that σ_1^* is a calculational quantity averaging the matrix strength in front of a major crack. Clear wood strength is less than σ_1^* .

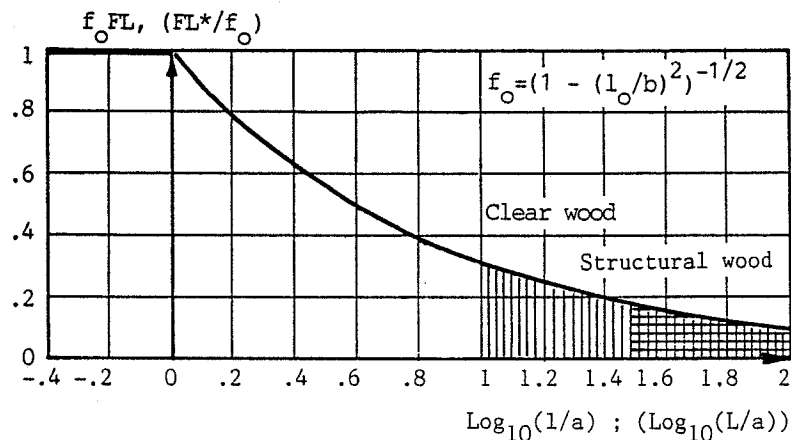


Figure 2.2. "Truncated" Griffith representation of strength levels for clear wood and structural wood (quantities in parenthesis). $a \approx .15 \text{ mm} < l \approx 1.5 \text{ mm} < L \approx 5 - 10 \text{ mm}$ are (half)sizes of defect nuclei, minor defect, and major defect respectively. Interaction factor, $f_0 = [1 - (l_0/b)^2]^{-1/2}$ where b is center distance between minor defects.

The strength level of structural wood ($L > 1$) is now given by Equations 2.5 and 2.7. We get

$$FL^* = \frac{\sigma_{\text{FL}}}{\sigma_1^*} = f_0^* \sqrt{a/L} \quad (2.8)$$

which is illustrated graphically in Figure 2.2.

For widely separated minor cracks ($a \approx 0.15 \text{ mm}$) and a single $2L = 10 \text{ mm}$ knot a strength level of $FL^* \approx 1/6$ for structural wood is predicted by Equations 2.8.

A remark should be made concerning the introduction of composite strength levels in viscoelastic crack mechanics: Both types of defects (minor and major) grow. This fact is of little practical importance when the relative change of K_{cr}^* is small. To check this the following relation is derived from Equation 2.6

$$\frac{1/K_{cr}^*}{K_{cr}^*} = \frac{n1}{l_0} \frac{(l_0/b)^2}{1 - (l_0/b)^2} = (f_0^2 - 1) \frac{n1}{l_0} \quad (2.9)$$

For example:

$$\frac{n1}{l_0} < 0.06 \quad ; (l_0/b < 0.8) \quad (2.10)$$

is required in the lifetime analysis of structural wood (non-local failure) when $l_0/b < 0.9$ ($f_0 < 1.67$) and $|K_{cr}^*/K_{cr}^*| < 0.1$ is required. The assumption is checked by a parallel clear wood analysis considering only the growth of minor cracks.

For this purpose

$$\frac{FL(\text{clear wood})}{FL(\text{struct. wood})} \approx f_0^{-2} \sqrt{L/l_0} \quad (2.11)$$

$$\frac{SL(\text{clear wood})}{SL(\text{struct. wood})} \approx \sqrt{l_0/L} \quad (2.12)$$

are derived from the expressions developed in this section. Equation 2.11 relates strength level of the clear wood fraction to strength level of composite (* = struct. wood). Correspondingly Equation 2.12 relates load level, $SL = \sigma/\sigma_{cr}$, of clear wood to load level of composite.

A practical notice: Index on FL and SL referring to clear wood and structural wood are omitted in the subsequent sections when the meaning is obvious from the text.

Chapter 3

Rheology of Wood

Practically the mechanical behavior of wood can be considered linear viscoelastic at loads lower than approximately 60 % of the ultimate strength. The creep function, $c(t)$, (strain developed by a unit stress applied at time, $t = 0$), is reasonably well described by the so-called Power Law,

$$c(t) = \frac{1}{E} (1 + a \cdot t^b) \quad (3.1)$$

In wood science Equation 3.1 is often referred to as the Clouser function since Clouser (17) was the first to suggest it for application to wood. The (dynamic) Young's modulus is denoted by E . The constant, $b \leq 1$, is dimensionless while the other constant, a , has a dimension of time to the power $-b$. The latter feature is, of course, somewhat unfortunate. A much more convenient equation for describing power law creep is

$$c(t) = \frac{1}{E} [1 + (\frac{t}{\tau})^b] \quad (3.2)$$

which has been considered in details by the present author in (18). The new constant, τ , has the significant meaning of defining the time at which the creep function has grown to twice its initial value. Because of that τ may be named the creep doubling time. Relaxation time, however, is a more appropriate name referring to common rheological terminology.

It was shown in (18) that creep as described by Equation 3.2 is associated with the following relaxation function, $r(t)$,

$$r(t) \approx \frac{1}{c(t)} = \frac{E}{1 + (t/\tau)^b} \quad (3.3)$$

when $b < 1/3$. The relaxation function describes the stress response when the material is exposed to a unit strain applied at $t = 0$. It is noticed that a 50 % stress reduction is predicted by Equation 3.3 when t equals the relaxation time, τ .

In subsequent sections considering viscoelastic crack mechanics it is convenient to operate with normalized versions of the creep function, $C(t)$, and the relaxation function, $R(t)$. Normalization is made with respect to the initial quantities. Thus

$$C(t) = 1 + (t/\tau)^b \quad (3.4)$$

$$R(t) \approx [1 + (t/\tau)^b]^{-1} \quad (b < 1/3) \quad (3.5)$$

3.1 RELAXATION TIME AND CREEP POWER

The following estimates from (18) on creep power and relaxation time may be applied when no experimental information are present. The estimates are based primarily on the authors inspection of information given in (17,19,20,21,22,23,24,25).

It was suggested in (18) that a creep power of size

$$b \approx 1/4 \quad (3.6)$$

is in general the best value for creep description of wood. The creep power can be considered practically independent of direction considered and temperature and humidity.

LOAD	LOG ₁₀ (τ , days)
tension, par.	5 \pm 1
bending, par.	4 \pm 1
compress. par.	3 \pm 1
shear, par.	3 \pm 1
tension, perp.	2 \pm 1

Table 3.1. Relaxation time for wood at equilibrium with normal climatic conditions; ($u \approx 15\%$, $T \approx 20^\circ\text{C}$). Parallel to grain and perpendicular to grain is denoted by par. and perp. respectively.

The relaxation time, however, is very dependent of direction and climatic conditions. The estimates in Table 3.1 apply at climatic equilibrium conditions at a temperature of $T = 20^\circ\text{C}$ and a moisture content (weight) of $u = 15\%$.

At climatic equilibrium conditions different from the reference conditions defined above, τ is modified (18) multiplying the reference τ with the following factor,

$$d = 10^{(15-u)/10 + (20-T)/15} \quad (3.7)$$

When less attention has been given to ensure equilibrium (dry conditions however), the τ -values will drop dramatically below their "equilibrium quantities"- eventually by a factor of 10^{-2} . At thin structural dimensions and severe climatic conditions (wet-dry) the τ -values will drop even more.

3.2 LOCAL RELAXATION TIME AT FAILURE

For plain opening and plain sliding modes it is shown in Appendix A (example 3) at the end of the article that local creep at a crack tip may be described approximately by a Clouser creep function with $b \approx 1/4$ and relaxation times as given in Table A.1.

LOAD	$\text{LOG}_{10}(\tau_{\text{ANA}}, d)$
tens	2.0 ± 1.0
sliding: bend	1.2 ± 1.0
compr	0.4 ± 1.0
opening	0 ± 1.0

Table 3.2. Local relaxation time at crack tip for plain opening mode and plain sliding mode.

This description of creep is based on a linear stress-strain response. It is, however, well-known that the stress-strain situation at the front of a crack is out of the linear range previously referred to. This means that the relaxation times given in Table A.1 are probably too high. No experimental data, however, are available considering creep in front of a propagating crack. Thus, an empirical reduction will be introduced which reflects the authors experience comparing experimental lifetime data with theoretically predicted data:

The special situation applying in the crack front area is considered approximately introducing an average relaxation time which is approximately 1/300 of the value expected in the linear stress-strain range. Table A.1 in Appendix A now reduces as shown in Table 3.2.

The overall failure model previously described in Section 2 predicts failure of wood to be a consequence primarily of cracks propagating along the grain in a combined opening mode and sliding mode fashion.

The composite relaxation time to be used in the failure model is considered in the subsequent text as a function of wood quality and loading mode.

3.2.1 CLEAR WOOD:

Tension parallel to grain:

A finger joint splintering type of failure will develop. Sliding primarily will characterize the local displacement, meaning

$$\log_{10}(\tau, \text{days}) \approx 2.0 \pm 1 \quad (3.8)$$

according to Table 3.2.

Compression parallel to grain:

Failure is initiated by a finger joint sliding just like in tension. At some point, however, coalesce of cracks will leave the fingers in an unstable position such that failure will proceed by wedge finger opening and overturning of fibers in a band perpendicular to grain.

The local displacement mode at a crack tip will then be a combination of sliding and opening. We suggest a square root average of the relaxation times given in Table 3.2. That is

$$\log_{10}(\tau, \text{days}) \approx 0.2 \pm 1 \quad (3.9)$$

Bending:

Bending is a combination of the two preceding cases. We may have a failure by compression or by tension. An appropriate average relaxation time is suggested which is

the square root average of τ from Equations 3.8 and 3.9. This means

$$\log_{10}(\tau, \text{days}) \approx 1.1 \pm 1 \quad (3.10)$$

LOAD	LOG ₁₀ (τ , days)
tension parall.	2 \pm 1
bending parall.	
compres.parall.	0 \pm 1
tension perp.	

Table 3.3. Clear wood (or local failure in structural wood).

Tension perpendicular to grain:

Failure is a result of cracks propagating in an opening mode. We have directly from Table 3.2

$$\log_{10}(\tau, \text{days}) \approx 0 \pm 1 \quad (3.11)$$

The "truncated" results obtained above for clear wood are summarized in Table 3.3.

LOAD	LOG ₁₀ (τ , days)
tension parall.	1 \pm 1
bending parall.	
compres.parall.	

Table 3.4. Structural wood with far reaching failure zones. At local failure use Table 3.3.

3.2.2 STRUCTURAL WOOD:

At long range failure patterns in structural wood it is unlikely that different relaxation times should apply for tension and compression parallel to grain. The bending quantity given in the Table 3.2 would here be a more reasonable estimate applying for any action (compression, tension, and bending) parallel to grain. Thus,

$$\log_{10}(\tau, \text{days}) \approx 1.2 \pm 1 \quad (3.12)$$

If knots influence the failure process only locally we expect a relaxation time similar to the clear wood quantity.

The "truncated" results obtained for structural wood are given in Table 3.4.

Chapter 4

Fatigue Analysis

The lifetime analysis presented in this section applies to a viscoelastic material weakened by a single crack. Generalization to multi-cracked materials is given in Section 5.

The elastic-viscoelastic analogy (also named the correspondence principle) (26,27) is the analytical basis. This analogy tells that a linear viscoelastic problem may be solved considering the solution to an elastic duplicate of the problem with identical dimensions, elasticity, external load, and internal stresses. All we have to do is to replace the elastic coefficients (Young's modulus f.ex.) with the corresponding viscoelastic operators (reciprocal creep function f.ex.).

When a non-decreasing load situation is considered there are no major problems in establishing an elastic counterpart to a Dugdale failure model of a cracked viscoelastic material. Due mainly to an assumption of identical coherent stresses at the crack front the two "counterparts" are automatically alike at any time.

When crack closure is present the problem of establishing elastic-viscoelastic counterparts is more complicated. Coherent stresses keep constant after crack closure when an elastic crack is considered. They relax in the case of a viscoelastic crack.

The principles of the present lifetime analysis are outlined as follows:

The assumption is made that a crack in a viscoelastic material is locked for some time after load reduction. Material pulled out into the crack front is stiff enough to oppose closing deformation. This viscoelastic crack situation can be looked upon by the elastic-viscoelastic analogy considering an elastic duplicate with time dependent (relaxing) stresses of coherence. It is justified in Appendix B at the end of the article that it is possible to construct such a fictitious elastic counterpart.

It is noticed that both counterparts have identical loads, crack lengths, and internal stresses. The coherent stresses are the time dependent ones just referred to.

The coherent stresses can only relax to a certain level from where on they keep constant. This level which is related to minimum load mainly defines the time at which the viscoelastic crack starts opening. This phenomenon is illustrated in Appendix B.

An illustration of corresponding elastic and viscoelastic crack front opening histories are shown in Figure 4.1.

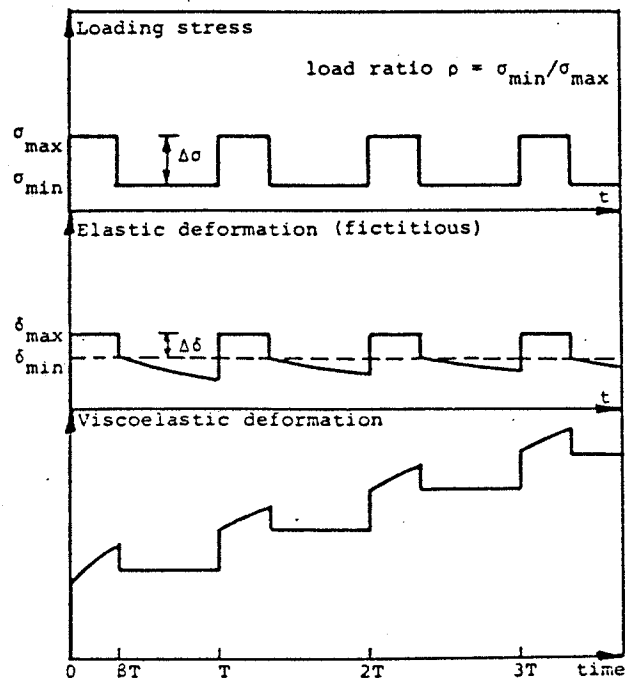


Figure 4.1. Corresponding elastic- and viscoelastic deformation histories.

Characteristic features are: a) the elastic opening closes (relaxes) when the viscoelastic opening keeps constant (locked), and b) the viscoelastic opening increases when the elastic opening is constant. The point of time at which behaviors a) and b) separate is the time mentioned above where the coherent stresses become constant.

Any movement, $\Delta\delta$, of the (viscoelastic) crack front is associated with an energy dissipation of size $|\Delta\delta \cdot \sigma_1|$. This is a consequence of assuming that the pulled out

crack front material is stiff and perfectly plastic with flow stress, $\pm\sigma_1$. The crack front becomes unstable when the integration of $|\dot{\Delta}\sigma_1|$ with respect to time becomes critical.

In order to establish the viscoelastic history of the crack front we need 1) solutions to the elastic crack closure problem, and 2) information on how in fact the crack opening counterparts considered above are related.

1) Solutions to the elastic crack closure problem have been obtained by the present author in (14) where high frequency fatigue lifetime of wood has been considered. Expressions relevant for the present study are summarized in the following Section 4.1.

2) Relations between the crack front counterparts are established in the subsequent Section 4.2.

As the latter point is considered mainly by introducing an average creep behavior of wood during the fatigue process we may in principle use exactly the same method for lifetime prediction as used when establishing the DVM-theory applying for non-decreasing load situations like deadload and rampload (e.g. 3).

This means: The crack moves a distance equal to the immediate crack front width, R , in a period of time, Ω , used to open the immediate crack tip to an extent where critical dissipation has been produced. The rate of crack propagation is then determined by R/Ω - and lifetime is predicted by integration to the point where the rate of propagation becomes infinite.

This point of analysis is considered in Section 4.3.

4.1 ELASTIC CRACK CLOSURE RELATIONS

Definitions and equations from (14) important for the present viscoelastic fatigue analysis are as follows. No theoretical explanation will be given.

$p = \sigma_{\min}/\sigma_{\max}$	(Load ratio)	
$SL_{\max} = \sigma_{\max}/\sigma_{CR}$	(Max. Load level)	
$SL_{\min} = \sigma_{\min}/\sigma_{CR}$	(Min. Load level)	(4.1)
$FL = \sigma_{CR}/\sigma_1$	(Strength level)	
$k = 1/l_0$	(Damage ratio)	

where σ_{cr} is (short time) strength and σ_1 is theoretical strength (equal to the materials flow stress previously considered at the crack front). Damage ratio is length, l , of running crack relative to the initial length, l_0 . Load varies periodically between σ_{MAX} and σ_{MIN} as shown in Figure 1.1.

Other expressions used in the analysis are

$$\begin{aligned} \Delta SL &= SL_{MAX} - SL_{MIN} = (1-p)SL_{MAX} \quad (\text{Load level range}) \\ k_{cr} &= l_{cr}/l_0 = SL_{MAX}^{-2} \quad (\text{Critical damage ratio}) \end{aligned} \quad (4.2)$$

where the critical damage ratio, k_{cr} , is the damage ratio at which damage rate becomes infinitely high.

The crack front width, R_{MAX} , and maximum crack front opening, δ_{MAX} , illustrated in Figure 1.2 are expressed by

$$R_{MAX} = \frac{\pi^2}{8} [SL_{MAX}FL]^2 \quad (4.3)$$

$$\delta_{MAX} = \frac{\pi \sigma_{MAX}^2}{E \sigma_1} - 1 = \frac{\pi}{E} [SL_{MAX}FL]^2 \quad (4.4)$$

Auxiliary expressions explained in (14) are the effective load ratio, p_{EFF} , and the efficiency factor, U , defined below. The location in the front zone at which the coherent stress changes dramatically is given by s_0 , see Figure 1.3.

$$p_{EFF} = 1 - [(1-p)U]^{M/4} [SL_{MAX}\sqrt{k}]^{(M/4 - 1)} \quad (4.5)$$

$$U = \frac{1}{2}(1 + p) \quad (4.6)$$

$$s_0 \approx 1 - \frac{C}{4}(1 - p_{EFF})^2 \quad (4.7)$$

where C is the so-called damage rate constant ($0 < C < 4[(1-p)U]^{-M/2}$). The damage rate power is M . For wood $(C, M) \approx (3, 9)$ were deduced in (14).

Front opening variation is given by

$$\frac{\delta_{MIN}}{\delta_{MAX}} \approx 1 - \frac{1}{2}(1 - p_{EFF})^2 \quad (4.8)$$

$$\Delta \delta \approx \frac{1}{2}(1 - p_{EFF})^2 \delta_{MAX} \quad (4.9)$$

Failure criterion is

$$\Gamma = \sigma_1 * \Sigma \delta \rightarrow \Gamma_{er} = \frac{K_{er}^2}{E} = \frac{\pi \sigma_{er}^2 l_0}{E} \quad (4.10)$$

Strength, $\sigma_{er,1}$, (residual strength) related to crack length:

$$\frac{\sigma_{er,1}}{\sigma_{er}} = \frac{1}{\sqrt{k}} \quad (4.11)$$

Theoretically the expressions given above apply only for a stretched material with widely separated cracks (i.e. crack center distance is larger than approximately 3 times the total crack length, $2*1$).

Practically, however, they also apply for multi-cracked materials subjected to compressive loads. Some minor modifications (on FL, SL, and U), however, have to be introduced. This feature is considered in Section 5.1.

4.2 ELASTIC-VISCOELASTIC COUNTERPARTS

The elastic-viscoelastic counterpart relation will be considered in two parts separated by $\delta(\text{elastic}) = \delta_{\text{MIN}}$ in Figure 4.1: a) The elastic part is a square wave deformation with maximum deformation, δ , and 0 minimum deformation (Figure 4.3), and b) the elastic part is a periodically varying "semi constant - semi relaxing" deformation where the constant is δ_{MIN} (Figure 4.2).

Part a) is considered in Section 4.2.2 introducing an amplification factor relating elastic and viscoelastic deformation.

Part b) is considered approximately in Section 4.2.1 introducing a so-called time shifted creep function applying to a "constant" elastic deformation of size δ_{MIN} .

4.2.1 TIME SHIFTED CREEP FUNCTION

Two situations are considered:

1) Constant crack closure: The elastic deformation is periodically constant over a period of time, βT , where T is the cyclic time. The viscoelastic deformation is periodically constant over the time, $(1-\beta)T$, where the

elastic counterpart varies. This situation is illustrated in Figure 4.2.

2) Partly crack closure: The two deformation histories start being related as in 1). At a certain time, however, the elastic part reaches a minimum at which it stays for the rest of the cycle. This minimum of relaxation is indicated by the factor H in Figure 4.2. An increasing viscoelastic deformation is the result of a constant elastic deformation.

An approximate method of relating the two deformations such defined is developed in the following by introducing a so-called time-shifted (or effective) creep function, $C_{eff}(t) = C(t/h)$, where $C(t)$ is the normalized creep function of the viscoelastic material considered and h is a constant.

The constant, h , will be determined using the present authors version of the so-called "E-effective method" (28) considering the time, T , of the first cycle.

The viscoelastic deformation between $t = 0$ and $t = \beta T$ is $y = C(\beta T)$. Considering especially $t = T$ we may express y also by means of the "E-effective method" such that

$$y = C(T) - \frac{E * \beta}{E_{eff}[(1-\beta)T]} = C(\beta T) \quad (4.12)$$

We have here determined y by subtracting the effect of the "triangular" elastic deformation growing from 0 at $t = \beta T$ to β at $t = T$ from the effect of a constant deformation of size 1.

The effective Young's modulus, E_{eff} , is given by

$$E_{eff}(t) = \frac{E}{1 + z * \phi(t)} \quad ; \quad z = \frac{1}{1 - R(t)} - \frac{1}{\phi(t)} \quad (4.13)$$

where the relaxation factor, z , is expressed by the normalized relaxation function, $R(t)$, and the creep factor, $\phi(t) = C(t) - 1$.

An assumption for the application of the "E-effective method" is that the elastic deformation involved must vary congruently with the creep function. This assumption is considered to apply sufficiently well in the present analysis.

In general the relaxation factor is time dependent. Practically, however, it can often be given a constant value. For example, concrete: $z \approx 3/4$, and wood: $z \approx 1$. Thus, for wood which is the main topic of the present article we have

$$E_{\text{eff}}(t) = E/C(t) \quad (4.14)$$

such that Equation 4.12 becomes

$$y = C(T) - n \cdot C((1-\beta)T) = C(\beta T) \quad (4.15)$$

which gives us

$$n_1 = \frac{C(T) - C(\beta T)}{C((1-\beta)T)} \quad (4.16)$$

Index 1 indicates that only deformation history 1) previously defined is considered by this expression.

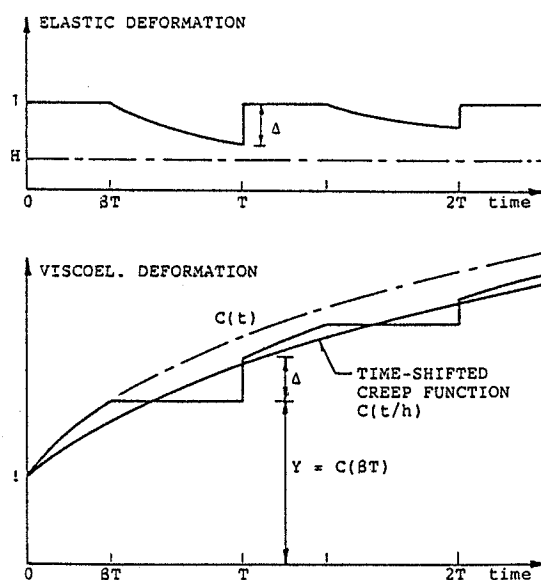


Figure 4.2. Auxiliary figure for determining an average creep function corresponding to the elastic deformation shown in the upper part of the figure.

When the elastic relaxation becomes so large that it tends to go below the lower bound, H , deformation history 2) becomes relevant. This means

$$n_2 = 1 - H \quad (4.17)$$

such that in total,

$$n = \min \left(\begin{matrix} n_1 \\ n_2 \end{matrix} \right) \quad (4.18)$$

which can also be written

$$n = \frac{1}{2} \{ 1 - H + n_1 - \sqrt{(1 - H - n_1)^2} \} \quad (4.19)$$

The shift factor, h, is now determined by

$$C(T/h) = y + n = C(T) - n*[C(1-\beta)T]-1]$$

such that

$$h = T/C^{-1}\{C(T) - n*[C(1-\beta)T]-1]\} \quad (4.20)$$

where $C^{-1}()$ is the inverse normalized creep function.

When Power Law creep especially is considered Equation 4.20 reduces as shown in the subsequent Equation 4.29.

4.2.2 VISCOELASTIC AMPLITUDE AMPLIFICATION

We consider the viscoelastic counterpart to a periodically varying square wave elastic deformation history, see Figure 4.3.

The average deformation is

$$y = \beta * C(t) \quad (4.21)$$

where t is time and $C(t)$ is the normalized creep function.

The elastic wave amplitude is 1. The corresponding viscoelastic amplitude (viscoelastic amplification factor), is G as shown in Figure 4.3.

The envelopes of the upper and lower amplitudes of the viscoelastic wave history are parallel to the average deformation. Thus,

$$G = C(\beta T) - \beta T \left(\frac{dy}{dt} \right)$$

or introducing Equation 4.21,

$$G = C(\beta T) - \beta^2 T \left(\frac{dC}{dt} \right)_{av} \quad (4.22)$$

The derivative refers to some average time in the period considered.

As G must be symmetric in β we also have

$$G = C([1-\beta]T) - (1-\beta)^2 T \left(\frac{dC}{dt} \right)_{av} \quad (4.23)$$

Assuming an arbitrary start of the wave loading we may consider the two derivatives in Equations 4.22 and 4.23 to be equal. Thus, the amplification factor may be obtained eliminating dC/dt between the two equations just mentioned. We get

$$G = \frac{(1-\beta)^2 C(\beta T) - \beta^2 C([1-\beta]T)}{1 - 2\beta} \quad (4.24)$$

When Power Law creep especially is considered we get the amplification factor given by the subsequent Equation 4.30.

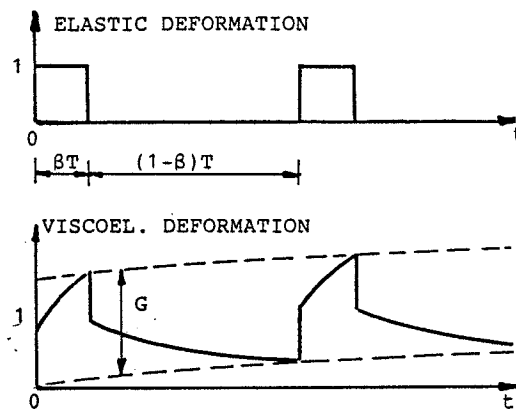


Figure 4.3. Viscoelastic amplitude amplification.

4.3 DAMAGE RATE

Following the procedure outlined in Section 4 we will now consider the energy dissipation produced when a position defined by the immediate crack tip is opened over a period of time, Ω , by crack penetration. The three contributions explained below are relevant in this context. Creep contributions are considered through the Power Law, Equation 3.4. The opening history shown in Figure 4.4 is "congruent" with the crack front profile given in Figures 1.1 and 1.3. This is a consequence of an assumption of a constant immediate damage rate.

$$\Gamma_1 = \delta_{MAX} [1 + (-\frac{\Omega}{qh\tau})^b] \sigma_1 - n\delta [1 + (-\frac{(1-s_w)\Omega}{qh\tau})^b] \sigma_1 \quad (4.25)$$

$$\Gamma_2 = \beta n\delta [1 + (-\frac{(1-s_w)\Omega}{q\tau})^b] \sigma_1 + (1-\beta)n\delta \sigma_1 \quad (4.26)$$

$$\Gamma_3 = G * \frac{1}{2} n\delta [2(1-s_w)\frac{\Omega}{T}] \sigma_1 = G * n\delta (1-s_w) \frac{\Omega}{T} \sigma_1 \quad (4.27)$$

Contribution 1:

Energy dissipation due to δ_{MIN} . Calculated as δ_{MAX} contribution minus $n\delta$ contribution.

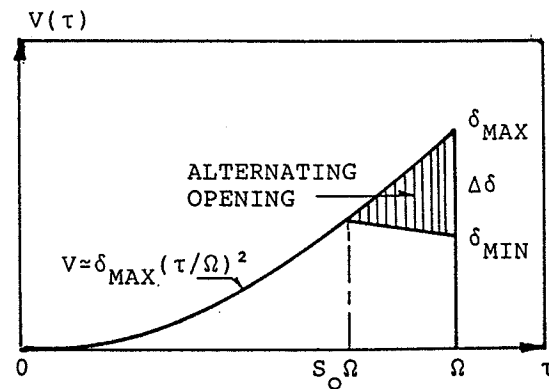


Figure 4.4. Opening history of a position being penetrated by a crack.

The parameter, q , is a factor considering that the position x which is penetrated by the crack does not experience the maximum crack opening at once (in which case $q = 1$). For a parabolically increasing opening history in a Power Law viscoelastic material q is developed in (3) as

$$q = [(1+b)(2+b)/2]^{1/b} \quad (4.28)$$

The parameter, h , considers the crack closure phenomenon by introducing a time shift in the creep function. For a Power Law material we get from Equations 4.16, 4.19 and 4.20

$$h = [1 - n*(1 - \beta)^b]^{-1/b} \quad (4.29)$$

$$n = \frac{1}{2} \{ 1 - H + n_1 - \sqrt{(1 - H - n_1)^2} \}$$

$$n_1 = \frac{1 - \beta^b}{(\tau/T)^b + (1-\beta)^b} ; \quad H \approx p^{b+1}$$

where H is a factor derived in Appendix B considering the state of maximum stress relaxation at the crack front.

Contribution 2:

Energy dissipation due to the average of the alternating opening (on top of the the δ_{MIN}).

Contribution 3:

This contribution considers energy dissipation directly produced by the opening alternation. The following viscoelastic amplification factor, G , on wave amplitude (relative to elastic value) is obtained by Equation 4.24 introducing Power Law creep,

$$G = 1 + \frac{\beta^b(1-\beta)^2 - \beta^2(1-\beta)^b}{1 - 2\beta} \left(\frac{T}{\tau}\right)^b$$

$$\rightarrow 1 + \frac{2-b}{2} \left(\frac{T}{2\tau}\right)^b \quad (\text{as } \beta \rightarrow 0.5) \quad (4.30)$$

Total dissipation:

The total energy dissipation is now given as follows when $\Omega\delta$ is introduced as given by Equation 4.9.

$$\frac{\Sigma\Gamma}{\delta_{MAX}\sigma_1} = 1 + \left[1 - \frac{1}{2}(1-p_{EFF})^2(1-s_0)^b(1-\beta h^b)\right] \left(\frac{\Omega/\tau}{qh}\right)^b$$

$$+ \frac{G}{2}(1-p_{EFF})^2(1-s_0)(\Omega/T) \quad (4.31)$$

or with $1-s_0$ from Equation 4.7

$$\frac{\Sigma\Gamma}{\delta_{MAX}\sigma_1} = 1 + \left[1 - \frac{C^b}{2^{1+2b}}(1-p_{EFF})^{2+b}(1-\beta h^b)\right] \left(\frac{\Omega/\tau}{qh}\right)^b$$

$$+ \frac{GC}{8}(1-p_{EFF})^4 \frac{\Omega/\tau}{T/\tau} \quad (4.32)$$

With δ_{MAX} from Equation 4.4 and introducing the failure criterion, $\Sigma\Gamma = \Gamma_{cr}$ from Equation 4.10 we get

$$\frac{1-kSL_{MAX}^2}{kSL_{MAX}^2} = \left[1 - \frac{C^b}{2^{1+2b}}(1-p_{EFF})^{2+b}(1-\beta h^b)\right] \left(\frac{\Omega/\tau}{qh}\right)^b$$

$$+ \frac{GC}{8}(1-p_{EFF})^4 \frac{\Omega/\tau}{T/\tau} \quad (4.33)$$

by which time to failure, Ω , of the position considered can be determined.

Over the same time the crack front has moved a distance equal to the immediate crack front width, R_{MAX} , given

by Equation 4.3. Crack velocity is then given by $dl/dt = R_{max}/\Omega$ which becomes

$$\frac{dk}{dt} = \frac{\pi^2}{8} \frac{FL^2}{\Omega} k SL_{max}^2 \quad (4.34)$$

introducing the damage ratio, $k = 1/l_0$.

When Ω is eliminated between Equation 4.33 and Equation 4.34 we get the following expression relating damage rate to damage ratio,

$$\begin{aligned} \frac{1 - k SL_{max}^2}{k SL_{max}^2} \left(\frac{dk}{dt} * \tau \right)^b = & \\ & \left[1 - \frac{C^b (1 - p_{eff})^{2+b} (1 - \beta h^b)}{2^{1+2b}} \right] \left(\frac{\pi^2 FL^2}{8qh} k SL_{max}^2 \right)^b \\ & + \frac{\pi^2 C * G * FL^2}{64(T/\tau)} k SL_{max}^2 (1 - p_{eff})^4 \left(\frac{dk}{dt} * \tau \right)^{b-1} \quad (4.35) \end{aligned}$$

Chapter 5

Generalizations

Following the assumptions previously made Equation 4.35 is immediately valid for stretched materials with widely separated cracks. From (10,11,14), however, may be concluded that the practical applicability of the expression is much broader. The following formulation on how to generalize the lifetime analysis with respect to multi-damage, arbitrary load ratio is reproduced from (14).

5.1 MULTI-DAMAGE SYSTEMS

A multi-crack system is considered with parallel, co-linear arrays of identical cracks of length $2l$ and equal center distance, $2b$. Distance between crack arrays is larger than $2b$.

The expressions previously obtained on the basis of a single-crack failure model can be generalized for the multi-crack situation just defined replacing strength level and load level according to

$$FL \Rightarrow f_0 FL \quad \text{and} \quad SL \Rightarrow f_1 SL \quad (5.1)$$

where the interaction factors, f_0 and $f_1 = f_1(k)$, are expressed by

$$f_0 = [1 - (\frac{l}{b})^2]^{-1/2} \quad (5.2)$$

$$f_1 = [f_0^2 - (f_0^2 - 1)k^2]^{-1/2} \quad (5.3)$$

where the damage ratio as usual is denoted by k . The interaction factor $f_0 \geq 1$ denotes how much stronger the multi-damaged material considered would have been with non-interacting damages ($f_0 = 1$).

The critical damage ratio at which damage rate approaches infinity becomes

$$k_{cr} = \frac{2f_0^2}{SL_{max}^2} [1 + \sqrt{1 + 4 f_0^2 (f_0^2 - 1) / SL_{max}^4}]^{-1} \quad (5.4)$$

5.2 ARBITRARY LOAD RATIO

The theory developed can be generalized to include negative load ratios by modifying the efficiency factor, U , from Equation 4.6 such that

$$U = \frac{1}{2}[1 + p + (\sqrt{p^2} - p)U_-] \quad (5.5)$$

where the minimum efficiency factor, $U(p=-1) = U_-$, is considered to be a materials constant.

The factor $H \approx p^{2.5}$ considers maximum relaxation in the time shift expression 4.29 at $p \geq 0$. It is suggested that negative load ratios can be considered introducing $H = 0$ which means that negative load ratios are expected to cause permanent crack closure. Thus,

$$H \approx [p - \frac{\sqrt{p^2}}{2}]^{2.5} \quad (5.6)$$

Chapter 6

Application
of Fatigue Theory

Lifetime is obtained by integration:

$$t_{CAT} = \int_1^{k_{CAT}} \frac{dt}{dk} dk \quad (6.1)$$

where k_{CAT} is the damage at which damage rate becomes catastrophically high. The inverse damage rate, dt/dk , is given by Equation 4.35.

It is noticed that Equation 6.1 does not include time to start of damage propagation. This feature, however, is of no practical importance. The contribution is very small (14) - and it is safe ignoring it.

Reduced strength is a result of fatigue increasing crack lengths. At the final failure situation strength has been reduced to $\sigma_{er}(N_{CAT}) = SL_{MAX} * \sigma_{er}$. During the fatigue period the residual strength, $\sigma_{er,r}$, of a multi-damaged material can be predicted by the following expression given in (14),

$$\frac{\sigma_{er,r}}{\sigma_{er}} = \left[\frac{f_0^2 - (f_0^2 - 1)k^2}{k} \right]^{1/2} = (f_1 \sqrt{k})^{-1} \quad (6.2)$$

with interaction factors, f_0 and f_1 , as defined in Equations 5.2 and 5.3. The special solution, Equation 4.11, applying to a single-damage situation is included with $f_0 = f_1 = 1$. The time dependent damage ratio, $k = k(t)$, is known from the numerical integration of Equation 6.1.

The residual critical stress intensity factor, $K_{er,r}$, varies according to Equation 2.6 with l_0 replaced by the increasing l . Thus,

$$\frac{K_{er,r}}{K_{er}} = f_0 \sqrt{1 - (l/b)^2} = \sqrt{f_0^2 - (f_0^2 - 1) * k^2} = f_1^{-1} \quad (6.3)$$

$K_{er,r}/K_{er}$ represents strength decrease due to a major defect introduced after preconditioning. Strength de-

crease of plain clear wood is still as predicted by Equation 6.2.

6.1 NUMERICAL BASIS

TYPE OF WOOD	MODE	FL (FL*)	LOG ₁₀ (τ, days)
Clear wood	tens(0)	$f_{\infty} * FL \approx$	2 ± 1
	bending(0)	$1/3$	1 ± 1
	compr(0)		0 ± 1
	tens(90)		0 ± 1
Struct. wood	tens(0)	$FL^*/f_{\infty} \approx$	1 ± 1
	bending(0)	$1/6 \rightarrow 0$	
	compr(0)		

Table 6.1. Estimates of strength level, FL, and relaxation time, τ . The interaction factor, f_{∞} , defined in Equation 2.3 has an order of magnitude 1 - 2. At increasing localized failure in structural wood the estimates approach the clear wood quantities. - Reference climate (equil. at moisture content, $u \approx 15\%$, and temperature, $T \approx 20^{\circ}\text{C}$). At a different equilibrium condition relaxation time is multiplied by the factor, $d = 10^{(15-u)/(10+(20-T)/10)}$.

A numerical procedure for prediction of lifetime, residual strength, and residual critical stress intensity factor is presented in Appendix C at the end of the paper. A summary is given on expressions needed for the analysis - and a FORTRAN program is generated considering multi-damaged materials subjected to fatigue loads with arbitrary mean (incl. negative).

Results of this numerical analysis are given in subsequent sections of the article.

The estimates of appropriate strength levels and relaxation times are based on Table 6.1 where information from Sections 2.1 and 3.2. are summarized. The program is open for any choice of creep power. However, for wood a value of $b = 0.25$ is always used. This has been justified previously.

Other basic fatigue parameters needed for a fatigue analysis of wood are the damage rate power, m , and the damage rate constant, C . Theoretically we may introduce any values for these parameters. However, to be consistent with the elastic fatigue theory developed in (14) we maintain from there $(m, C) = (9, 3)$.

Normally clear wood problems are considered by the multi-damage theory. This means that the interaction factor, f_0 (through f_1 , see Equation 5.3), is continuously integrated in the analysis.

Most often structural wood is sufficiently well considered by the more simple single-damage theory. Here the interaction factor, f_0 , is used only for estimating strength level. (If, for some reason, a multi-damage analysis would be appropriate with major defects of size $2L$ separated by a distance, $2B$, then the interaction factor in the calculational part of the program given in Appendix C is given the value $F_0 = (1 - (L/B))^{-1/2}$. For estimating strength level FL^*/f_0 in Table 6.1 is replaced by $FL^*/(f_0 * F_0)$).

It should be noticed that strength level for structural wood is not always denoted by FL^* in the following. When the meaning is evident from the text we only write FL .

Useful controls on the results of lifetime calculations are the following special results:

Deadload lifetime at load \equiv maximum load:

Progressing damage, k , under dead-load at $SL \equiv SL_{max}$ (and the corresponding residual strength) is of interest when evaluating the lower frequency results of a fatigue analysis. The basic expression applying for single-damaged materials is the following developed in (3)

$$\frac{dk}{dt} = \frac{FL^2}{W * \tau} \frac{kSL^2}{[(1/(kSL^2)) - 1]^{1/b}} \quad (6.4)$$

The constant, W , is given by

$$W = (8/\pi^2)[(1+b)(2+b)/2]^{1/b} \quad (6.5)$$

Residual strength is

$$\frac{\sigma_{er}(t)}{\sigma_{er}} = 1/\sqrt{k} \quad (6.6)$$

For $b = 0.25$ especially Equation 6.4 can be solved analytically. We get the following expression relating damage ratio and time,

$$FL \frac{t}{\tau} = \frac{3.2}{SL^2} \left[-\frac{1-k^{-4}}{4SL^2} - \frac{4(1-k^{-2})}{3SL^4} + \frac{3(1-k^{-2})}{SL^4} - \frac{4(1-k^{-1})}{SL^2} + \log_e(k) \right] \quad (6.7)$$

Lifetime, t_{DEAD} , is obtained by this expression introducing the critical damage ratio, $k_{cr} = 1/SL^2$. We get

$$FL \frac{t_{DEAD}}{\tau} = \frac{3.2}{SL^2} \left[\frac{Y^4}{4} - \frac{Y^3}{3} + \frac{Y^2}{2} - Y - \log_e(SL^2) \right] \quad (6.8)$$

with $Y = 1/SL^2 - 1$. Equation 6.8 is shown graphically in Figure 6.1.

Equation 6.4 can be generalized to include multi-damage systems applying a procedure suggested in Section 5.1.

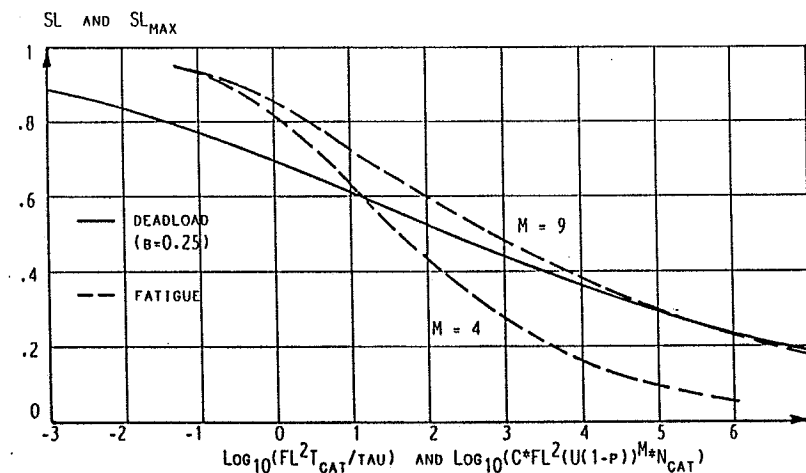


Figure 6.1. Deadload lifetime, t_{DEAD} , at $SL \equiv SL_{MAX}$, with creep power, $b = 0.25$, and high frequency fatigue lifetime number of cycles at $m = 4$ and 9 .

Elastic fatigue lifetime:

Progressing damage, k , under elastic fatigue (high frequency loading) and the corresponding residual strength) is of interest when evaluating the higher frequency results of a fatigue analysis. The basic ex-

pression applying for single-damaged materials is the following developed in (14)

$$\frac{dk}{dN} = \frac{\pi^2 C}{64} FL^2 \frac{[U \cdot nSL]^m}{1 - kSL_{max}^2} k^{m/2} \quad (6.9)$$

where the efficiency factor, U , is given by Equation 5.5.

For a single crack situation Equation 6.9 can be solved analytically giving the following relation between damage ratio and number of cycles. The result is

$$N \frac{C \cdot FL^2}{[U(1-p)]^{-m}} = \frac{13}{SL_{max}^m} \left[\frac{1 - k^{1-(m/2)}}{m-2} - \frac{1 - k^{2-(m/2)}}{m-4} SL_{max}^2 \right] \quad (6.10)$$

The residual strength is then given by Equation 6.6 above.

Fatigue lifetime number of cycles, N_{CAT} , is obtained introducing the critical damage rate, $k_{cr} = 1/SL^2$, into Equation 6.10. We get

$$N_{CAT} \frac{C \cdot FL^2}{[U(1-p)]^{-m}} = \frac{13}{SL_{max}^2} \left[\frac{1 - SL_{max}^{2-m}}{2-m} - \frac{1 - SL_{max}^{4-m}}{4-m} \right] \quad (6.11)$$

which is shown graphically in Figure 6.1 with $m = 4$ and 9.

Equation 6.9 can be generalized to include multi-damage systems applying a procedure suggested in Section 5.1.

6.2 EXPERIMENTS AND THEORY

As far as high frequency loading concerns experimental justification of the theory presented has already been given in (14). The present section therefore concentrates on fatigue lifetimes at moderate and low load frequencies.

The author only knows of one experimental work, namely (1), where a systematic examination has been made to describe the fatigue phenomenon of wood as related to load frequency. Small clear spruce specimens were subjected to square wave loading parallel to grain at five frequencies between 0.1 Hz and 10^{-3} Hz. A load ratio of $p = 0$ was applied with a fractional time at maximum

minor cracks has grown to a size (fex. $2l = 4$ mm) such that some average model between clear wood and structural wood would be appropriate. No information, however, is available which can explain the "real" model. (From Equation 2.8: $FL^*/f_m \approx \sqrt{(0.15/2)} \Rightarrow FL^* = 0.4$ with $f_m \approx 1.5$). The theoretical results shown in Figure 6.2 are based on the single-damage model.

Realizing that much more experimental data are needed in the field of fatigue of wood the present author and Borg Madsen designed a program for tensile fatigue testing of small clear Douglas-Fir specimens perpendicular to grain (radially). Data from sine wave and square wave loading at arbitrary frequencies, $f \leq 1$ Hz should supplement the observations of Bach and in addition give information on the unknown influence on fatigue of load ratio, $p = SL_{MIN}/SL_{MAX}$, and fractional time, β , under maximum load.

The test specimens developed were small rectangular specimens, $(R,L,T) = 14*4*1.75$ cm³, with a centrally placed RL tunnel crack of length, $2l = 1$ cm. Load is transferred by wire to eye bolts attached to the center of 4 mm steel plates glued to the specimen ends.

The test equipment designed for less than 0.1 Hz square wave experiments was based on the "multi-member rack" previously developed by Borg Madsen et al. at the University of British Columbia (e.g. 6); A number of specimens are suspended from mountings attached to the top of a glulam beam. Each specimen is loaded from below through a wire attached at one end to the specimens eyebolt and at the other end to a lever arm whose fulcrum is attached to the beam bottom. Load is controlled fixing a weight to the appropriate location on the lever arm.

In order to cope with arbitrary values of p and β the multi-member rack was modified such that an up and down moving table deactivates and activates respectively according to a programmable time schedule the lower of two lever arm weights suspended in series.

The 1 Hz sine load experiments (with variable p) were planned to be run on a high precision, electronically controlled fatigue apparatus (Bob Gray design).

However, due to unforeseen difficulties in obtaining financial support the project could not be completed as planned. The only results obtained (29,30) are data from pilot tests run to check the test set ups: 1) Sine load fatigue at $p = 0$, - 2) 0.001 Hz square wave fatigue at $(p, \delta) = (0, 0.5)$, and - 3) deadload (in multi member rack).

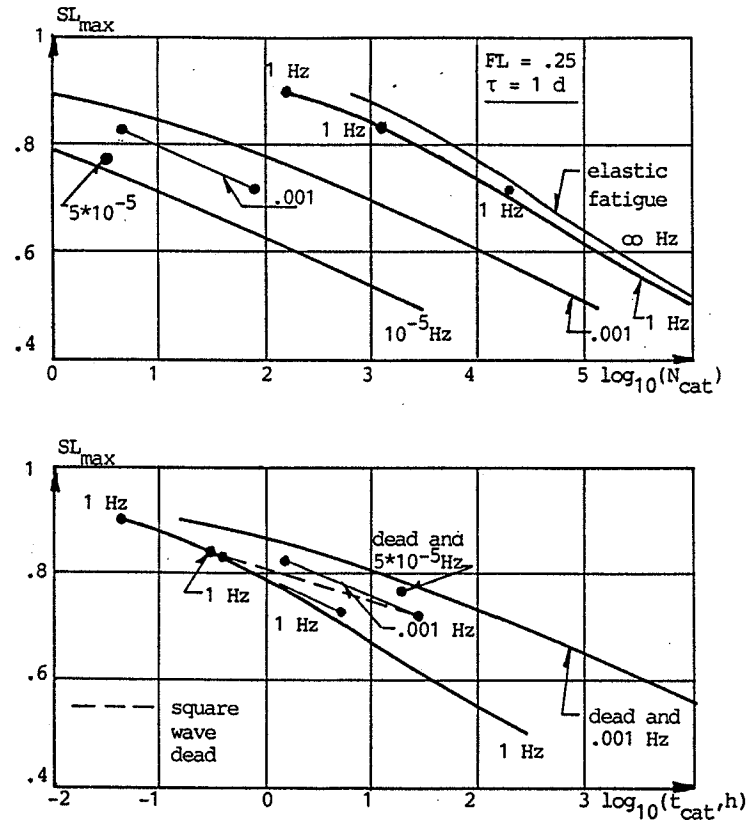


Figure 6.3. Fatigue lifetime and deadload lifetime of Douglas-Fir loaded perpendicular to grain with a load ratio of $p = SL_{min}/SL_{max} = 0$. Experimental data from (29,30,6). Heavy lines are theoretical results obtained as explained in the main text.

Due to the lack of resources two features have to be considered carefully when evaluating the results obtained: 1) All experiments were related to strength control data measured on the Bob Gray apparatus mentioned above, and 2) most experiments were started several months after the control tests such that appropriate references may have shifted somewhat due to climatic changes (and storing conditions). These features

will be commented on along with the following summary of the results obtained;

The 1 Hz (sine) tests were made at $\sigma_{\max} = 1.96, 2.25$ and 2.56 MPa. The respective number of cycles to failure were $\log_{10}(N_{\text{CAT}}) \pm \text{s.d.} = 4.27 \pm 0.42[19], 3.06 \pm 0.76[20],$ and $2.22 \pm 1.22[19]$ where sample size is given in parenthesis.

The 0.001 Hz and deadload tests were made at $\sigma_{\max} = 1.93$ and 2.23 MPa. The respective number of cycles to failure were $\log_{10}(N_{\text{CAT}}) \pm \text{s.d.} = 1.92 \pm 1.21[20]$ and $0.68 \pm 0.91[30]$. The deadload lifetimes were $\log_{10}(t_{\text{CAT}}, \text{hours}) \pm \text{s.d.} = 1.44 \pm 0.93[20]$ and $-0.41 \pm 1.73[28]$.

A strength control test (with the 10 mm crack) was made (on the Bob Gray apparatus) with the result: $\sigma_{\text{cr}} = 2.95 \pm \text{s.d.} 0.23$ MPa[31].

Preparation of all specimens, strength control, and half of the upper load ($\sigma_{\max} = 2.56$ MPa) sine tests were made under normal room climatic conditions in the winter time. The major part of the experiments, however, had to be postponed almost half a year. During this period of time the reference strength decreased by $\approx 10\%$. This is observed comparing the max. load sine "winter results" with the "summer results". 1/3 of the latter were b.o.l. (broke on loading) results. None of the "winter results" were b.o.l. data. The observation that a strength reduction had occurred is supported by a "summer" strength control test giving $\sigma_{\text{cr}} = 2.72 \pm \text{s.d.} 0.23$ MPa[8]. The material for this control was originally saved and intended for another purpose (residual strength during a fatigue process). It was preconditioned, before introducing the 1 cm crack, with 5000 cycles to $\approx 55\%$ of its (uncracked) strength - a preconditioning which can be anticipated only to reduce strength insignificantly.

A third indication that strength reduction had occurred during the spring is found considering the max. load deadload lifetime data. Here $\approx 20\%$ of the sample size broke on loading. This indicate a $\approx 20\%$ reduction. Probably, however, the extra 10 % is due to difference in test equipment.

Except for the 2.56 MPa 1 Hz result all data presented in Figure 6.3 from (30,31) refer to stress levels based on $\sigma_{cr} = 2.72$ MPa (summer result). For the exception an average, $\sigma_{cr} = 2.84$ MPa, of the winter and summer strength is used.

Also shown in Figure 6.3 is a single 5×10^{-3} Hz result (square wave load, $\beta \approx 1/3$) and a single deadload result from tests by McDowal (6, exp. 4) on specimens similar to those previously described. Hour glass shapes, however, were used with neck width, $2b = 2.5$ cm, and crack length, $2l = 0.6$ cm. The tests were made at $\sigma = 1.90$ MPa with $\sigma_{cr} = 2.47 \pm 0.20$ MPa [17]. Average fatigue lifetime of sample size 28: $\log_{10}(N_{CAT}) \approx 0.5$. Average deadload lifetime of sample size 27: $\log_{10}(t_{CAT}, \text{hours}) \approx 1.3$.

The theoretical graphs of Figure 6.3 are obtained by the single-damage theory presented in the article with $(p, \beta) = (0, 0.5)$, $FL^* = 0.25$, and $\tau = 1$ day. The latter quantities are estimated from Table 6.1 considering the test specimens as made of artificial structural wood: $FL^*/f_0 = 1/6$ with $f_0 = 1.5$ and τ from clear wood, tension perp. (The crack sizes used in the experiments are not different enough practically to justify different strength levels - and the crack length to specimen width = 0.25 is not big enough practically to justify a multi-damage analysis).

6.3 FATIGUE PREDICTIONS

Three examples will now be given on how we may predict the influence of varying loads on 1) residual strength in structural wood, 2) residual critical stress intensity factor for clear wood, and 3) lifetime of structural wood.

The latter example considers three types of fatigue loading: Tension with $(p, \beta) = (0, 0.5)$, Peak tension with $(p, \beta) = (0, 0)$, Peak-released deadload tension with $(p, \beta) = (0, 1)$ and reversed bending with $(p, \beta) = (-1, 0.5)$.

Finally the threshold (or endurance limit) phenomenon is discussed in a separate section.

6.3.1 RESIDUAL STRENGTH

Figure 6.4 shows some results of a residual strength analysis of structural wood exposed to fatigue tension with $SL_{\max} = 0.5$, fractional time under loading, $\beta = 0.5$, and load ratio, $p = 0$. A single-damage model and Equation 6.2 is used for the analysis with a strength level of $FL^* = 0.25$ and a relaxation time of $\tau = 10$ days. ($FL^*/f_0 = 1/6 \Rightarrow FL^* = 0.25$ with $f_0 = 1.5$).

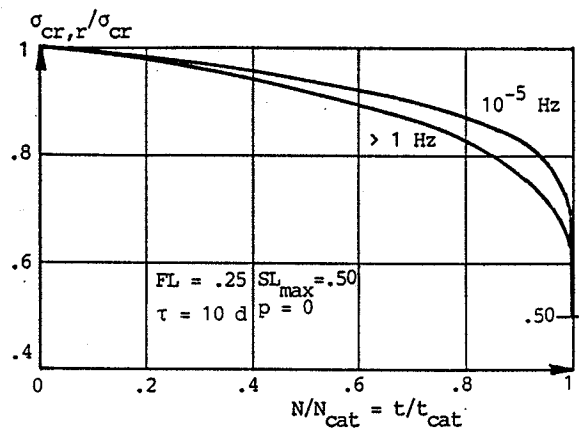


Figure 6.4. Residual strength of structural wood exposed to tension fatigue. Predictions as described in the main text.

The upper graph in Figure 6.4 applies for a frequency of 10^{-5} Hz. The lower curve applies at 1 Hz - and practically for any frequency higher than that.

A residual strength expression valid for deadloading has previously been developed by the author in (11,II). It yields (with creep power, $b = 0.25$)

$$\frac{\sigma_{cr,r}}{\sigma_{cr}} \approx \sqrt{SL^2 + (1 - SL^2)(1 - [t/t_{DEAD}])^{1/4}} \quad (6.12)$$

the results of which practically coincide with the 10^{-5} Hz graph in Figure 6.4.

6.3.2 RESIDUAL CRIT. STRESS INTENSITY FACTOR

Figure 6.5 demonstrates the influence on the critical stress intensity factor, K_{cr} , of preconditioning clear wood perpendicular to grain with a number of square

wave load cycles with $SL_{MAX} = 0.55$ and load ratio, $p = 0$. Relative time under maximum load is $\beta = 0.5$. A multi damage model and Equation 6.3 is used with $FL = 0.15$, $f_o = 1.5$, and $\tau = 1$ day.

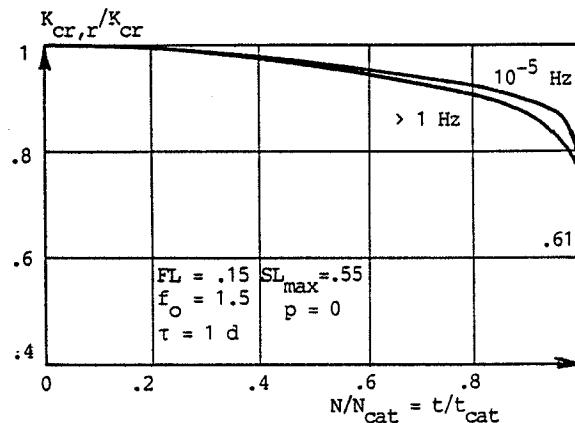


Figure 6.5. Residual critical stress intensity factor of clear wood exposed to tension fatigue perpendicular to grain. Predictions as explained in main text.

It is noticed from Figure 6.5 that strength reduction due to fatigue first becomes significant when half the time to failure has past. This justifies the statement previously made that no significant strength loss is present after 5000 cycles at a load level of 0.55.

6.3.3 LIFETIME AS RELATED TO LOAD FREQUENCY

In the following examples lifetime is predicted for structural wood loaded parallel to grain as defined by various combinations of p and β .

In general a strength level of $FL^* = 0.25$ ($FL^*/f_o = 1/6$ with $f_o = 1.5$) is assumed together with a relaxation time of $\tau = 10$ days.

Tension with $(p, \beta) = (0, 0.5)$:

The results of a lifetime study for this case are shown in Figures 6.6 and 6.7. In the former figure lifetime is expressed by number of cycles to failure. In the latter figure time to failure is given in real time.

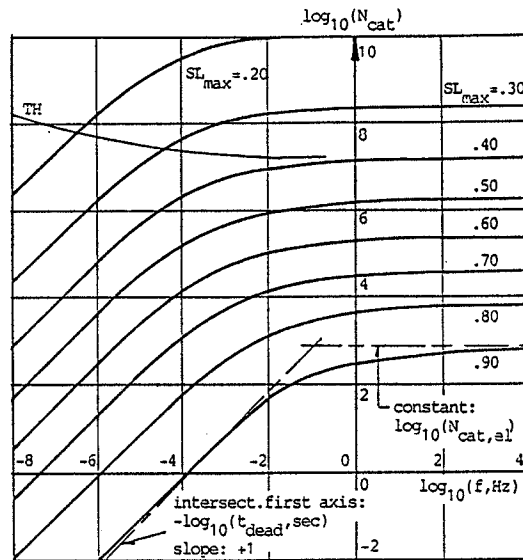


Figure 6.6. Number of cycles to failure in structural wood subjected to a periodically varying tensile load with $(p, \beta) = (0, 0.5)$. A time to failure presentation of data is given in Figure 6.7. Estimates indicated at $SL_{max} = 0.9$ are explained in Section 6.3.4. Thin line indicates a threshold (TH) on load level below which no fatigue failure will ever occur; see Section 6.3.5.

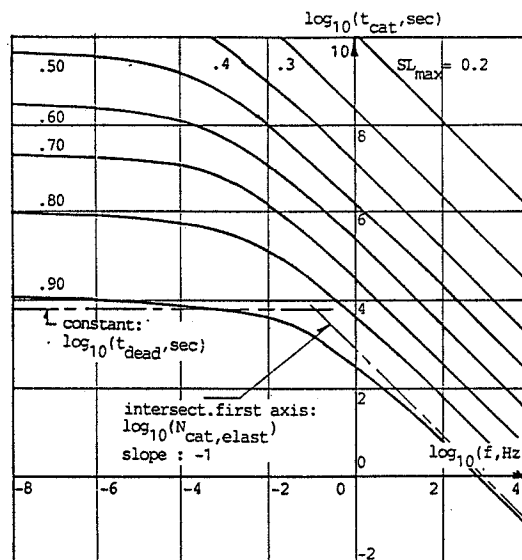


Figure 6.7. Time to failure in structural wood subjected to a periodically varying tensile load with $(p, \beta) = (0, 0.5)$. A number of cycles presentation of data is given in Figure 6.6.

The thin lines theoretical data at $SL_{max} = 0.9$ indicate deadload and elastic fatigue "estimates" by Equations 6.8 and 6.11 respectively. It is noticed that lifetime at low frequencies only has increased insignificantly relative to the one predicted at deadload. At higher frequencies lifetime is practically equal to the elastic fatigue lifetime. The transition area is approximately 4 decades wide. Somewhat dependent on load level the center of transition is located at frequencies 10^{-4} - 1 Hz.

Also shown in Figure 6.6 is a threshold estimate based on a hypothesis explained later in Section 6.3.5.

Tension with $(p, \beta) = (0, 1)$ and $(0, 0)$:

These tensile loading types are very extreme. The former corresponds to "peak-released deadload" (deadload periodically released very shortly to 0). The latter denotes a periodic "peak load" with 0 in between. Some results of the analysis are shown in Figure 6.8.

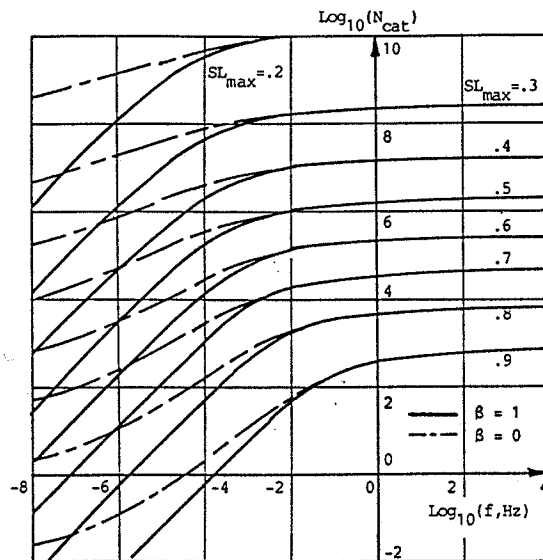


Figure 6.8. Number of cycles to failure in structural wood subjected to a periodically varying tensile load; a) Peak load, $(p, \beta) = (0, 0)$, and b) peak-released deadload, $(p, \beta) = (0, 1)$.

At low frequencies the peak released deadload lifetime is slightly lower than deadload lifetime. Similar over-

all trends, however, applies as for the lifetime description in Figure 6.6.

At low frequencies the peak load lifetime is significantly longer than the one applying for peak released deadload. This is a result of a smaller effective creep inducing load. (It should be mentioned that creep effects are still present at peak load situations. They are introduced indirectly by stress relaxation at the crack front).

Reversed bending, $(p, \beta) = (-1, 0.5)$:

As an example this type of loading is obtained exposing a rectangular beam to a moment which varies periodically between + and - M. The lifetime results are shown in Figure 6.9.

Similar lifetime trends are observed as in Figure 6.6. However, elastic fatigue lifetime is smaller, and the transition center has shifted to lower frequencies

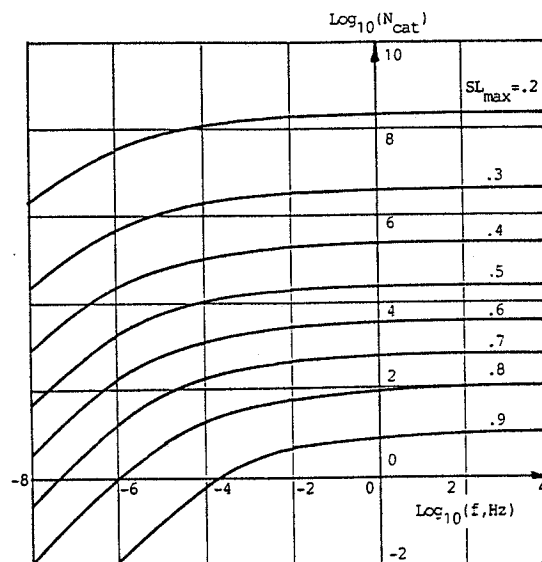


Figure 6.9. Number of cycles to failure in structural wood subjected to reversed bending with $(p, \beta) = (-1, 0.5)$.

6.3.4 ON ESTIMATES AND LIFETIME PRESENTATION

For $\beta > \approx 0.4$ a numerical evaluation of the lifetime theory developed shows that lifetime diagrams for practice may be constructed very easily using the deadload

failure solution, t_{DEAD} , and elastic fatigue failure solution, N_{CAT} , expressed by Equations 6.8 and 6.11 respectively. The method of construction is outlined below - and to some extent illustrated in Figure 6.6 at $SL_{MAX} = 0.9$.

The two straight lines are drawn representing deadload failure and elastic fatigue failure. The intersection point defines the center of an approximately 4 decades wide transition area where lifetime goes from being influenced mainly by creep to be influenced primarily by the elastic fatigue process. Lifetime in the transition area is described by a straight line truncating symmetrically the intersection corner.

Real frequency used as independent variable is somewhat inconvenient. A more adequate first axis unit would be a dimensionless frequency, $\underline{f} = f \cdot \tau$, producing a second axis unit of dimensionless time, $\underline{t} = t / \tau$. Following the above considerations on lifetime prediction when $\beta > \approx 0.4$ we now get,

NUMBER OF CYCLES ESTIMATE:

$$\begin{aligned} N_{CAT} &= f \cdot t_{DEAD} = (f \cdot \tau) \cdot (t_{DEAD} / \tau) = \underline{f} \cdot \underline{t_{DEAD}} && ; (\text{low } f) \\ N_{CAT} &= N_{CAT,EL} && ; (\text{high } f) \end{aligned}$$

In a log-log representation we get:

$$\begin{aligned} \log_{10}(N_{CAT}) &= \log_{10}(\underline{t_{DEAD}}) + \log_{10}(\underline{f}) && ; (\text{low } f) \\ \log_{10}(N_{CAT}) &= \log_{10}(N_{CAT,EL}) && ; (\text{high } f) \end{aligned} \quad (6.13)$$

Transition area is constructed as previously indicated in this section.

TIME ESTIMATE:

$$\begin{aligned} t_{CAT} &= N_{CAT,EL} / f = (N_{CAT,EL} \cdot \tau) / (f \cdot \tau) \Rightarrow \\ t_{CAT} &= N_{CAT,EL} / \underline{f} && ; (\text{high } f) \end{aligned}$$

and

$$\begin{aligned} t_{CAT} &= t_{DEAD} = \tau \cdot (t_{DEAD} / \tau) \Rightarrow \\ t_{CAT} &= \underline{t_{DEAD}} && ; (\text{low } f) \end{aligned}$$

In a log-log representation we get:

$$\begin{aligned} \log_{10}(t_{CAT}) &= \log_{10}(N_{CAT,EL}) - \log_{10}(\underline{f}) && ; (\text{high } f) \\ \log_{10}(t_{CAT}) &= \log_{10}(\underline{t_{DEAD}}) && ; (\text{low } f) \end{aligned} \quad (6.14)$$

Again the transition area is constructed as previously indicated.

It is important to notice that non-dimensional lifetime representations according to the above considerations practically make design N_{CAT} -diagrams independent of relaxation time, τ .

We have not used non-dimensional data representation in the examples of Section 6.3.3. Practically we therefore have to shift the $\log_{10}(N_{CAT})$ graphs presented 1 decade to higher frequencies when $\tau = 1$ day in stead of 10 days.

6.3.5 THRESHOLD

There are many speculations on the existence of a threshold on load alternation below which no fatigue failure will ever occur in wood. No experimental evidence, however, is present at the time being which significantly supports the threshold idea. Thus, the following should be considered as an hypothesis which gives a mechanistic explanation on the phenomenon if it exists.

In (14) an expression was developed which predicts a load range threshold below which no elastic fatigue failure will ever occur. The expression is based on the assumption that a crack will stop propagating if the number of cycles needed for propagating a distance equal to the immediate crack front zone width, R , exceeds a certain critical number, N_{TH} , by which "cyclic hardening" of the crack front material blunts any attempt of further propagation.

For fatigue in general of viscoelastic materials we now rephrase this criterion such that a threshold state is defined if the rate of predicted number of cycles to failure, $N_{CAT,PR}$, exceeds a critical value which is given by its elastic counterpart determined in (14). For $(SL_{MAX}, SL_{MIN}) = (SL, 0)$ this means that fatigue failure will not occur if

$$\frac{N_{CAT,PR}}{k_{er}} = N_{CAT,PR} * SL^2 > N_{CAT,EL} * SL_{TH}^2 \quad (6.15)$$

where k_{er} is the critical damage ratio given by Equation 4.2 and $N_{CAT,EL}$ is the elastic fatigue number of

cycles to failure given by Equation 6.11 for the (elastic) threshold load level, SL_{TH} .

For example: For a tensile load variation we read from (14, Section 6.5) $SL_{TH} \approx 0.40$ which corresponds to $N_{CAT,EL} \approx 10^{7.2}$, see Figure 6.6. Thus, by Equation 6.15 no fatigue failure occurs when

$$N_{CAT,FR} * SL^m > 10^{6.4} \quad (6.16)$$

This criterion is indicated in Figure 6.6 by a thin line. We notice for example that a $SL = 0.3$ situation always provokes failure at frequencies, $f < \approx 10^{-4.5}$ Hz.

Chapter 7

Conclusions and Final Remarks

A DVM (Damaged Viscoelastic Materials) theory previously developed by the author applies well when predicting deadload lifetime of wood. This has been shown in a number of articles.

A further developed DVM theory has recently (14) been shown also to explain successfully existing experimental data on fatigue failure of wood at very high frequencies (elastic fatigue).

In a way two extremes of the fatigue mechanical behavior of wood are hereby described; - 1) Extremely low frequency loading where creep of wood is the dominant cause of time dependent break down of structure, and - 2) Extremely high frequency loading where creep has no time to be of significance. The overriding strength reducing effect in this frequency area is due to energy dissipation produced by frequent tensile-compressive alternating deformations of material close to damages.

In the present work these descriptions of wood mechanical behavior are "linked" such that fatigue lifetime can be predicted at more realistic load frequencies where structural break down is a consequence of an integrated energy dissipation process involving both creep and crack closure effects. In addition to lifetime the theory also predicts residual quantities of strength and critical stress intensity factor as a consequence of progressing fatigue damage.

Very few tests are known which consider the influence of creep on the fatigue lifetime of wood. Thus, at the time being only a limited amount of experimental verification can be given of the theory presented. However, strong supports for the theory are found in the 1 Hz and $5 \cdot 10^{-4}$ Hz test data shown in Figures 6.2 and all the data in Figure 6.3. (The discrepancy between theoretical data and the 0.001 Hz experimental results shown in Figure 6.2 is probably due to a false refer-

ence strength of the latter data. This has been commented on in Section 6.2).

In general a lifetime and residual strength analysis by the theory needs to be made on a computer. An exception, however, applies when load variations are considered with fractional time under maximum load, $\beta > \approx 40\%$. For such cases lifetime graphs may be constructed very easily as shown in Section 6.3.4. At low frequencies lifetimes are predicted only to differ insignificantly from deadload lifetimes (at $SL \equiv SL_{max}$).

At decreasing fractional time under maximum load, $\beta < 0.4$, lifetimes become increasingly larger than the corresponding deadload lifetime. At the extreme peakload situation, $(p, \beta) = (0, 0)$, a factor of 10 is the order of magnitude when frequency is $f = 1$ peak per 10 days.

When lifetime is known residual strength and residual critical stress intensity factor at low frequency loading can be estimated by Equation 6.12.

7.1 FINAL REMARKS

It has been mentioned that only a few experimental works are reported in the literature where a systematic examination has been made of the influence of load frequency on fatigue life of wood. The few references, however, indicate without any doubt that such an influence exists and that it is strong. The present work identifies creep being responsible for this behavior.

It is noticed from the figures of Section 6.3.3 that low and moderate load frequencies, $f \leq 1$ Hz, are of special interest in the study of wood fatigue because they characterize the area of transition from high frequency, elastic fatigue to areas of strongly creep influenced fatigue failures.

Future experimental work on fatigue of wood must therefore include tests similar to those designed by the author and Borg Madsen (described in Section 6.2) - and tests with positive-negative load variations should be added. No sufficiently detailed understanding of the failure mechanism of wood can be obtained without such research.

ACKNOWLEDGMENTS

The work reported is part of a research project, "The Mechanical Durability of Wood", carried out at the Building Materials Laboratory, Technical University of Denmark and the Civil Engineering Department, Timber Engineering Section, University of British Columbia (UBC), Vancouver, B. C., Canada. The project has been supported by these institutions, privately, and by the Danish Technical Research Council (StvF-16-3785.B-172).

The author acknowledges especially the many and giving discussions he had with professor Borg Madsen (UBC) during the work.

LITERATURE

- 1) Bach, L.: "Frequency-Dependent Fracture under Pulsating Loading". Build. Mat. Lab., Techn. Univ. Denmark, Technical Report 68(1979). (Presented at Forest Prod. Res. Society Annual Meeting, Portland, Oregon, U.S.A., 15. June 1975).
- 2) Nielsen, L. Fuglsang: "On the Concept of Wood behaving like a Cracked Linear-Viscoelastic Material". IUFRO-Engineering Group Meeting, Madison, Wi., USA, June/July 1983. Proc. IUFRO S5.02, Dept. Civ. Eng., Univ. British Columbia, Vancouver, B. C., Canada, 1983, 103.
- 3) Nielsen, L. Fuglsang: "A Lifetime Analysis of Cracked Linear Viscoelastic Materials - with Special Reference to Wood". IUFRO-Engineering Group Meeting, Borås, Sweden 1982. Proc. IUFRO S5.02, Chalmers Univ. of Technology, Dept. Civil Eng., Gothenburg 1982, 151-178. (Also Techn. Rep. 92/80, Build. Mat. Lab., Techn. Univ. of Denmark, Copenhagen, 1980).
- 4) Nielsen, L. Fuglsang: "Crack Failure of Dead, Ramp, and Combined Loaded Viscoelastic Materials". First Int. Conf. on Wood Fracture, Banff, Alberta, Canada, August 1978. Proc., 1979, Western Forest products Lab., Univ. Brit. Columbia, Vancouver, B. C., Canada, 187-200.
- 5) Nielsen, L. Fuglsang and Hoffmeyer, P.: "Lifetime of loaded Wood - Viscoelastic Crack Theory", (in danish). Techn. report 149/85, (final report on StvF project 16-1816.B-865). Build. Mat. Lab., Techn. Univ. Denmark, Copenhagen 1985.
- 6) McDowal, B. J.: "The Duration of Load Effects in Tension Perpendicular to the Grain for Douglas Fir". Thesis 1982, Dept. Civ. Eng., Univ. Brit. Columbia, Vancouver, B. C., Canada
- 7) Johns, K. and Madsen B.: "Duration of Load Effects in Lumber. Part I; A Fracture Mechanics Approach". Can. J. Civ. Eng., 9(1982), 502-514.
- 8) Madsen, B. and Johns, K.: "Duration of Load Effects in Lumber. Part II; Experimental Data". Can. J. Civ. Eng., 9(1982), 515-525.
- 9) Madsen, B. and Johns, K.: "Duration of Load Effects in Lumber. Part III; Code Considerations". Can. J. Civ. Eng., 9(1982), 526-536. (Discussion by Foschi, R. O. and the authors of Part I, II and III of the paper in Can. J. Civ. Eng. 10(1983), 317-323).

- 10) Nielsen, L. Fuglsang: "On the Mechanical Behavior of Materials with Interacting Cracks". IUFRO-Engineering Group Meeting, Borås, Sweden 1982. Proc. IUFRO S5.02, Chalmers Univ. of Technology, Dept. Civil Eng., Gothenburg 1982, 141.
- 11) Nielsen, L. Fuglsang: "Wood as a Cracked Viscoelastic Material", "Part I: Theory and Applications" and "Part II: Sensitivity and Justification of a Theory". International Workshop on Duration Of Load, 12.-13. sept. 1985, Vancouver, B. C., Canada. Proc. FORINTEK, Western Forest Products Lab., Vancouver, B. C., Canada, Special Publication No. SP-27, 1986, Part I: 67-78, Part II: 79-89.
- 12) Nielsen, L. Fuglsang and Kousholt, K.: "Stress-Strength-Lifetime Relationship for Wood". Wood Science, 12(1980), 162-164.
- 13) Dugdale, D. S.: "Yielding of Steel Sheets containing Slits". J. Mech. and Phys. of Solids, 8(1960), 100-104.
- 14) Nielsen, L. Fuglsang: "Elastic Fatigue of Wood and other Building Materials". Building Materials Lab., Techn. Univ. Denmark. Techn. Rep. 170A(1986).
- 15) Rice, J. R.: "Mechanics of Crack-Tip Deformation and Extension by Fatigue". Fatigue Crack Propagation, ASTM STP 415(1967), 247-311.
- 16) Schniewind, A. P. and Lyon, D. E.: "A Fracture Mechanics Approach to the Tensile Strength Perpendicular to Grain of dimension Lumber". Wood Science and Technology, 7(1973), 45-59.
- 17) Clouser, W. S.: "Creep of small Wood Beams under constant Bending Load". U.S. Forest Products Lab., Report 2150(1959).
- 18) Nielsen, L. Fuglsang: "Power Law Creep as related to Relaxation, Elasticity, Damping, Rheological Spectra and Creep Recovery - With Special Reference to Wood". IUFRO-Engineering Group Meeting, Xalapa, Mexico, December 1984. Proc. Techn. Univ. Denmark, Build. Mat. Lab., Copenhagen 1984, 181-204.
- 19) Krebs, H. J.: "The Influence of Moisture Content on the Long Term Mechanical Properties of Wood" (in danish). Thesis 1984. Build. Mat. Lab., Techn. Univ. of Denmark. Chapter 5.
- 20) Nielsen, L. Fuglsang and Hoffmeyer, P.: "Lifetime of loaded Wood - Viscoelastic Crack Theory", (in danish). Techn. report 149/85, (final report on StvF project 16-1816.B-865). Build. Mat. Lab., Techn. Univ. Denmark, Copenhagen 1985.

- 21) Gressel, P.: "Zur Vorhersage des langfristigen Formänderungsverhaltens aus Kurz-Kriechversuchen". Holz als Roh- und Werkstoff, 42(1984), 293-301.
- 22) Nielsen, A.: "Long-time Deflection of Wood Beams". (in danish). Nordisk Trætidsskrift (Aalborg University Center, Denmark), 7(1981), 201-210.
- 23) Schniewind, A. P. and Barrett, J. D.: "Wood as a linear Orthotropic Viscoelastic Material". Wood Science and Technology, 6(1972), 43-57.
- 24) Kass, A. J.: "Inelastic Mechanical Behavior in Wood stressed perpendicular to the Grain radially". Thesis, Agriculture, Wood Technology, Univ. of Michigan, USA, 1969.
- 25) Kingston, R. S. T. and Budgen, B.: "Some Aspects of the Rheological Behavior of Wood, Part IV", Wood Science and Technology, 6(1972), 230-238.
- 26) Alfrey, T.: "Non-Homogeneous Stresses in Viscoelastic Media". Qu. Appl. Math. 2(1944), 113.
- 27) Flügge, W.: "Viscoelasticity". Blaisdell Publishing, London 1967.
- 28) Nielsen, L. Fuglsang: "Constitutive Equations for Concrete". Bygningsstatistiske Meddelelser (Copenhagen), 45(1974), 65.
- 29) Nielsen, L. Fuglsang and Gray, R.: "1 Hz Fatigue of Douglas-Fir perpendicular to Grain". Unpublished data. Dept. of Civ. Eng., Univ. Brit. Columbia, Vancouver, B. C., Canada 1984.
- 30) Nielsen, L. Fuglsang and Madsen, Borg: "Fatigue at low and moderate load frequencies of Douglas-Fir perpendicular to grain". Unpublished data. Dept. of Civ. Eng., Univ. Brit. Columbia, Vancouver, B. C., Canada 1984.

APPENDIX A

ON ORTHOTROPIC CRACK MECHANICS

OVERALL SYSTEM

We consider a crack in wood considered as a plane isotropic material where the plane of orthotropy is a cross-section perpendicular to grain. Any direction in this section is referred to by subscript S. The normal of the plane is parallel to grain and will be referred to by subscript L.

Common subscripts in the literature on wood technology are L, R and T meaning longitudinal, radial and tangential direction respectively referring to the real polar symmetrically orthotropic structure of wood. The properties in the RT-plane (cross-section) can, however, be averaged for most practical purposes. A very appropriate average is obtained by $X_{\text{RT}} = \sqrt{(X_{\text{R}} * X_{\text{T}})}$ where X_{R} and X_{T} symbolize corresponding elastic coefficients in the radial and tangential direction respectively. Subscript "S" represents the average quantity in this note.

ELASTICITY

The following orders of magnitudes for the elastic coefficients of wood may be deduced from the literature (e.g. 1):

$$\begin{aligned} E_{\text{S}}/E_{\text{L}} &\approx G_{\text{LS}}/E_{\text{L}} \approx 0.06 \text{ (softwood)}; \approx 0.08 \text{ (hardwood)} \\ \mu_{\text{LS}} &\approx \mu_{\text{SS}} \approx 0.4 \text{ (softwood)}; \approx 0.5 \text{ (hardwood)} \end{aligned}$$

where index i on Young's modulus, E, refers to extensional stress in the i-direction. Index ij on Poisson ratio, μ , refers to strain in j-direction for extensional strain in the i-direction (Poisson ratios are related by $\mu_{i,j}/E_i = \mu_{j,i}/E_j$). On shear modulus, G, subscript ij refers to shear in the ij-plane.

A derived elastic coefficient is the shear modulus, $G_{\perp\perp}$, perpendicular to grain,

$$G_{\perp\perp}/E_L = \frac{E_{\perp\perp}/E_L}{2(1 + \mu_{\perp\perp})} \quad ; (\approx 0.02) \quad (\text{A.1})$$

Some examples of parallel to grain Young's moduli, E_L , are (e.g. 2):

Softwoods: Spruce, Pine and Doug.-Fir have $E_L \approx 11500$, 16000 and 16500 MPa respectively.

Hardwoods: Birch, Ash, Beech have $E_L \approx 16500$, 16000 and 14000 MPa respectively.

CRACK SYSTEMS

The three crack systems shown in Figure 1 are considered: The SL-system, the LS-system, and the SS-system. First system symbol refers to normal direction of crack plane. The second symbol indicates direction of crack extension.

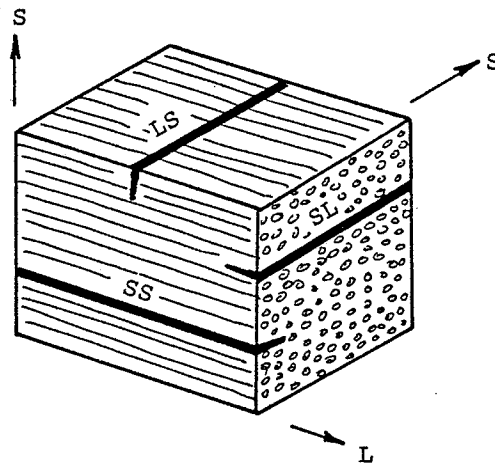


Figure A.1. Plane isotropic material and crack systems considered. For wood: L is direction along the grain. S is any cross grain direction. An IJ-crack has an I-directed crack plane normal and extends in the J-direction.

All three situations can be analyzed by the crack equations applying to isotropic materials. Only the Young's modulus has to be replaced by an analogy modulus, E_{ANA} , given as follows. Numbers in parenthesis refer to ave-

rage elastic coefficients for wood as given in the preceding section. (The analogy moduli here presented are from (3) where they were generated on the basis of (4,5,6)).

SL-CRACK - CRACK EXTENSION ALONG THE GRAIN

Opening mode (Mode I, plane stress):

With the following abbreviations

$$\alpha = \left(\frac{E_L}{E_B}\right)^{1/4} \quad ; (\approx 2.0) \quad (A.2)$$

$$\beta = \frac{1}{2} \left(\frac{E_L}{G_{LB}} - 2\mu_{LB} \right) * \sqrt{\frac{E_B}{E_L}} \quad ; (\approx 2.0) \quad (A.3)$$

the analogy modulus for a SL-crack becomes

$$E_{ANA} = E_B * \alpha * \sqrt{\frac{2}{1 + \beta}} \quad ; (\approx 1.6 * E_B) \quad (A.4a)$$

$$\approx 2E_B * [(E_B/G_{LB}) + 2\sqrt{E_B/E_L}]^{-1/2} \quad (A.4b)$$

where the latter expression applies at $G_{LB} \ll E_L$ (which is the case for wood).

Sliding mode (Mode II):

$$E_{ANA} = E_L * \frac{1}{\alpha} * \sqrt{\frac{2}{1 + \beta}} \quad ; (\approx 0.4 * E_L) \quad (A.5a)$$

$$\approx 2E_L * \sqrt{E_B/E_L} * [(E_B/G_{LB}) + 2\sqrt{E_B/E_L}]^{-1/2} \quad (A.5b)$$

where the latter expression applies at $G_{LB} \ll E_L$ (which is the case for wood).

Tearing mode (mode III):

$$E_{ANA} = 2 * \sqrt{G_{LB} G_{BB}} \quad ; (\approx 1.2 * G_{LB}) \quad (A.6)$$

LS-CRACK - CRACK EXTENSION PERP. TO GRAIN

Strictly speaking this system is rarely relevant for wood because the orthotropic strength distribution in this material does not allow cracks crossing grain except at impact loading. An apparent LS-crack in wood is mostly a result of fibers (or bundles of fibers) being

pulled out by local shear failures leaving a rough "LS" failure surface.

Opening mode (Mode I, plane stress):

$$E_{ANA} = E_L * \frac{1}{\alpha} * \sqrt{\frac{2}{1 + \beta}} \quad ; (\approx 0.41 * E_L) \quad (A.7a)$$

$$E_{ANA} \approx 2E_L * \sqrt{E_B/E_L} * [(E_B/G_{LB}) + 2\sqrt{E_B/E_L}]^{-1/2} \quad (A.7b)$$

where the latter expression applies at $G_{LB} \ll E_L$ (which is the case for wood).

Sliding mode (Mode II):

$$E_{ANA} = E_B * \alpha * \sqrt{\frac{2}{1 + \beta}} \quad ; (\approx 1.6 * E_B) \quad (A.8a)$$

$$E_{ANA} \approx 2E_B * [(E_B/G_{LB}) + 2\sqrt{E_B/E_L}]^{-1/2} \quad (A.8b)$$

where the latter expression applies at $G_{LB} \ll E_L$ (which is the case for wood).

Tearing mode (mode III):

$$E_{ANA} = 2 * \sqrt{G_{LB} G_{BB}} \quad ; (\approx 1.2 * G_{LB}) \quad (A.9)$$

The similarity between the SL-crack system and the LS-system should be noticed. Only the mode I and mode II expressions have been interchanged.

BB-CRACK - CRACK EXTENSION SIDEWAYS TO GRAIN

Opening mode (Mode I, plane stress):

$$E_{ANA} = E_B \quad (A.10)$$

Sliding mode (Mode II):

$$E_{ANA} = E_B \quad (A.11)$$

Tearing mode (mode III):

$$E_{ANA} = 2G_{LB} \quad (A.12)$$

CRACK PARAMETERS

Two parameters are of special interest when looking at materials failure: The strain energy release rate, Γ ,

and the stress intensity factor, K . The two quantities are related by

$$\Gamma = K^2/E_{ANA} \quad (A.13)$$

Failure occurs when Γ (and K) approach their critical values,

$$\Gamma_{cr} = K_{cr}^2/E_{ANA} \quad (A.14)$$

Every crack system and failure mode is associated with a characteristic crack parameter.

There is only a very limited amount of comparable (test methods and climatic conditions) data on crack parameters in the literature of wood science. Some orders of magnitudes, however, can be estimated on the basis of (7) for example:

Cracks not crossing grain (SL- and SS-systems):

$$K_{I,cr} \approx 300 - 600 \text{ kPa}\sqrt{\text{m}}$$

$$K_{II,cr} \approx 5 \cdot K_{I,cr}$$

Cracks "crossing grain" (LS-system):

$$K_{I,cr} \approx 10 \text{ times the SL- and SS quantities}$$

Data given in the literature considering cracks crossing grain (LS-systems) especially are very scattered. This is probably a result of the phenomenon previously mentioned that cracks in wood rarely cross grain in a direct way, meaning that test results are difficult to interpret.

EXAMPLES

EXAMPLE 1:

A Mode I test on a SL-crack system in Douglas-Fir reveals a critical stress intensity factor, $K_{cr} = 400 \text{ kPa}\sqrt{\text{m}}$. Also given by test is a Young's modulus, $E_w = 1000 \text{ MPa}$. What is the corresponding critical strain energy release rate, Γ_{cr} ? The answer is obtained by Equations A.4a and A.14. We get

$$\begin{aligned}\Gamma_{cr} &\approx K_{cr}^2 / (1.6 E_S) \\ &= 1000 \text{ J/m}^2\end{aligned}\quad (\text{A.15})$$

which is the energy applied in the process of a 1 m extension of the SL-crack considered.

For comparison: When a "LS-crack" system is considered in mode I with $K_{cr} = 4000 \text{ kPa}\sqrt{\text{m}}$ and $E_L = 16500 \text{ MPa}$ the result becomes $\Gamma_{cr} = K_{cr}^2 / (0.4 E_L) = 2500 \text{ J/m}^2$.

EXAMPLE 2:

The crack opening displacement (COD), δ , of a mode I crack in an isotropic material (with Young's modulus E) is given by

$$\delta = \frac{\pi \sigma^2}{E \sigma_1} l \quad (\text{A.16})$$

where σ is load and σ_1 is theoretical strength. Crack (half)length is l .

Introducing the failure condition, $\delta \Rightarrow \delta_{cr}$, strain energy release rate, $\Gamma = \delta \sigma_1$, becomes critical at $\Gamma_{cr} = \delta_{cr} \sigma_1$ such that Equation A.16 now predicts strength, σ_{cr} , of the cracked material. We get

$$\sigma_{cr} = \sqrt{\frac{E \Gamma_{cr}}{\pi l}} \quad (\text{A.17})$$

In wood with a SL-crack system COD is given by Equation A.16 replacing E with $E_{SNA} \approx 1.6 * E_S$ from Equation A.4a. We get

$$\delta_S \approx 0.6 \frac{\pi \sigma^2}{E_S \sigma_{1,S}} l \quad (\text{A.18})$$

where δ_S and $\sigma_{1,S}$ denote COD and theoretical strength respectively in the S-direction. Strength in the same direction, $\sigma_{cr,S}$, is predicted by

$$\sigma_{cr,S} \approx 1.3 * \sqrt{\frac{E_S \Gamma_{cr,S}}{\pi l}} \quad (\text{A.19})$$

with critical strain energy release rate in the S-direction, $\Gamma_{cr,S} = \delta_{cr,S} * \sigma_{1,S}$.

EXAMPLE 3:

We consider a SL-crack in wood. How does the crack opening displacement, COD, develop with time when the

viscoelasticity is characterized by the following creep functions,

$$C_i(t) = 1 + \left(\frac{t}{\tau_i}\right)^{1/4} \quad (\text{A.20})$$

where t is time and τ_i ($i = L, S, LS$) is relaxation time as estimated from the following table reproduced from the main text of the article;

LOAD	LOG ₁₀ (τ , days)
tension, par.	5 \pm 1
compress. par.	3 \pm 1
shear, par.	3 \pm 1
tension, perp.	2 \pm 1

Opening mode (mode I, plane stress):

The time dependent COD is determined by Equation A.16 replacing $1/E$ with $(1/E_{ANA}) * C_{ANA}(t)$ where $C_{ANA}(t)$ is the composite creep function obtained by Equation A.4b replacing $1/E_{ANA}$ with $(1/E_{ANA}) * C_{ANA}(t)$ and any $1/E_i$ with $(1/E_i) * C_i(t)$.

For $E_S/E_L \approx G_{LS}/E_L \approx 0.06$ and relaxation times given by the table given above we get (for both compression and tension quantities of τ)

$$C_{ANA}(t) \approx 1 + \left(\frac{t}{\tau_{ANA}}\right)^{1/4} \quad (\text{A.21})$$

with

$$\text{LOG}_{10}(\tau_{ANA}, \text{days}) \approx 2.5 \quad (\text{A.22})$$

by which the time dependent COD is determined as indicated above.

Sliding mode (mode II):

A similar procedure applies for the mode II situation. By means of Equation A.5b we get a creep function similar to the one described by Equation A.21. The relaxation time, however, is dependent whether the compression- or the tensile τ quantity is used. We get

$$\text{Log}_{10}(\tau_{\text{ANA}}, \text{days}) \approx 2.9 \quad (\text{compression}) \quad (\text{A.23})$$

$$\text{Log}_{10}(\tau_{\text{ANA}}, \text{days}) \approx 4.5 \quad (\text{tension}) \quad (\text{A.24})$$

The (log)average may be estimated for bending. This means

$$\text{Log}_{10}(\tau_{\text{ANA}}, \text{days}) \approx 3.7 \quad (\text{bending}) \quad (\text{A.25})$$

The results obtained above are summarized in Table A.1. It should be emphasized that the quantities given are based on linear crack analysis. In practice smaller values apply at the highly stressed crack tips. An empirical modification considering this feature is presented in the main text of the paper.

LOAD	LOG ₁₀ (τ_{ANA}, d)
tens	4.5 ± 1.0
sliding: bend	3.7 ± 1.0
compr	2.9 ± 1.0
opening	2.5 ± 1.0

Table A.1. Crack opening relaxation times for SL cracks in clear wood considered as a perfectly elastic material.

LITERATURE - APPENDIX A

- 1) Hearmon, R. F. S.; "Elasticity of wood and plywood". Dept. Sci. Indus. Res., Forest Products Research, Special report No. 7, HMSO, London 1948.
- 2) U.S. Forest Products Lab.; "WOOD Handbook; Wood as an Engineering Material". Agricultural Handbook No. 72 (revised). U.S. Government Printing Office, Washington, D. C., 1974. (Seasoning of Wood; Chapt. 14-4).
- 3) Nielsen, L. Fuglsang; "A Lifetime Analysis of Cracked Linear Viscoelastic Materials - with Special Reference to Wood". IUPRO-Engineering Group Meeting, Borås, Sweden 1982. Proc. IUPRO S5.02, Chalmers Univ. of Technology, Dept. Civil Eng., Gothenburg 1982, 151-178. (also available as Techn. Rep. 92/80, Build. Mat. Lab., Techn. Univ. of Denmark, Copenhagen, 1980).
- 4) Stormont, C. W., Gonzalez, H. and Brinson, H. F.; "The Ductile Fracture of Anisotropic Materials". Experimental Mech., 12(1972), 557-563.

- 5) Cottrell, A. H.: "Mechanism of Fracture". First Tewksbury Symp. on Fracture, Univ. of Melbourne, Australia, August 1963, Proc., Butterworth & Co. Ltd., Melbourne 1965.
- 6) Sih, G. C. and Liebowitz, H.: "Mathematical Theories of Brittle Fracture", in "Fracture" (ed. Liebowitz, H.), II, 67. Academic Press, New York, London 1968.
- 7) Wright, K. and Leppävuori E.: Application of Fracture Mechanics: Fracture Toughness of Finnish Wood". Technical Research Center of Finland, Lab. of Struct. Eng., 1985 ?.

APPENDIX B

ON VISCOELASTIC CRACK CLOSURE

SCOPE

The scope of this appendix is to demonstrate that it is possible to construct an elastic crack closure situation which - by the elastic-viscoelastic analogy - produces a viscoelastic counterpart with a "locked" crack front. This means that the front of a crack in a viscoelastic material is invariable for some time after a load reduction. In other words, the relaxation of coherent stresses is considered at a locked crack front in a viscoelastic material.

As a special case the present analysis includes the elastic crack closure phenomenon first considered by Rice (1). The results obtained do not agree totally with the results of Rice. This is due mainly to a different assumption of the coherent stress distribution at the crack front - and slightly to an approximate crack opening expression introduced in the analysis. However, no differences of principal and practical importance are observed.

The latter remarks are made in order not to compare too rigorously single results from this appendix with single results from the main text of the present article which, to some extent, is based on the results of Rice.

The present analysis assumes (like the Rice analysis) that no crack surface contact is present outside the crack front area.

ANALYSIS

We consider a crack centrally placed in an infinite linear-viscoelastic sheet uniformly loaded at infinity perpendicular to the crack plane. A model of such a

crack is shown in Figure B.1 together with some symbols and definitions often referred to in the subsequent text.

The load, σ , varies from a maximum of σ_{MAX} to a minimum of σ_{MIN} defined by the load ratio,

$$P = \sigma_{MIN}/\sigma_{MAX} \quad (B.1)$$

We assume that crack tip coherence is due to pulled out material exhibiting stiff, perfectly plastic behavior with yield stresses $\pm\sigma_1$.

The crack front opening (see Figure B.1) is invariable for some time after load reduction. The pulled out material locks for further deformation until the coherent stresses have relaxed beyond consistency with a "frozen" crack front.

The statement of an invariable crack opening can be looked upon applying the elastic-viscoelastic analogy which relates corresponding elastic solutions and viscoelastic solutions. For the present problem it is appropriate to formulate the analogy by

$$v_{visc} = \int_{-\infty}^t C(t - \theta) \frac{dv}{d\theta} d\theta \quad (B.2)$$

where t is a time and $C(t)$ is the normalized creep function of the viscoelastic material (Young's modulus, E , times the real creep function, $c(t)$). v_{visc} is viscoelastic crack opening considered while v is its counterpart in an exact elastic duplicate of the viscoelastic crack problem (Young's modulus, load, time, length and coherent stresses at the crack front).

As long as we have a frozen crack opening Equation B.2 reduces as follows,

$$v_{visc} = \int_{-\infty}^t C(t - \theta) \frac{dv}{d\theta} d\theta = \text{Constant} \quad (B.3)$$

This relation forms the basis of the present analysis the primary scope of which is to get an idea of what coherent stresses are associated with viscoelastic crack closure - and when does a closed crack start opening again.

Three principal steps are involved in the analysis (not necessarily considered in the following order);

- 1) An elastic analysis of relations in general between crack tip deformation and state of coherence.
- 2) A sorting out of deformations which are consistent with Equation B.3. The time at which the crack starts opening again is given when consistency cannot be found.
- 3) The latter step automatically produces the coherent stresses (as they are identical with the elastically determined stresses).

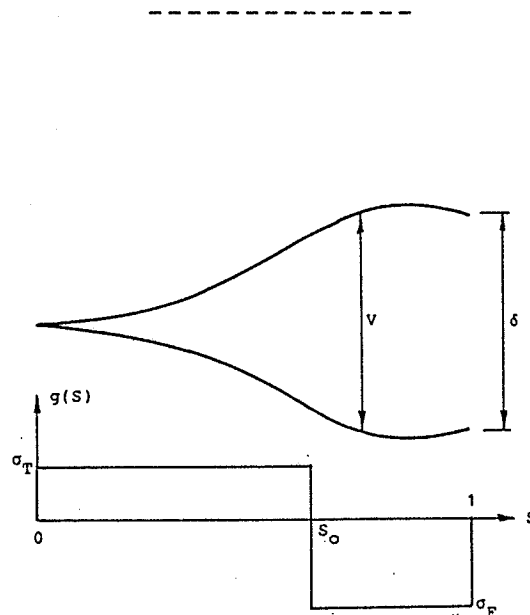


Figure B.1. Crack front. Relative location coordinate is s such that $s = 1$ corresponds to crack front width, R . Stress of coherence, $g(s)$. Crack opening, $v(s)$. Front opening, δ .

The following "elastic" equations relating crack front shape to external load and internal stress of coherence, can be established using the crack theory of Barenblatt (2) for example;

The width, R , of the crack front is given by

$$R = \frac{\pi K_{II}}{2} \left[\int_0^1 \frac{g(\tau)}{\sqrt{\tau}} d\tau \right]^{-2} \quad (\text{B.4})$$

where K is the stress intensity factor and $g(s)$ is stress of coherence as a function of the relative location coordinate, s , defined in Figure B.1.

The crack opening is given by

$$v = v_I + v_V \quad (\text{B.5})$$

where v_V and v_I expressed below are opening components produced by external load and internal load, $g(s)$, respectively

$$v_V = \frac{8R}{\pi E} \int_0^1 \frac{g(\tau)}{\sqrt{\tau(s)}} d\tau = \frac{8K}{E} \sqrt{\frac{R}{2\pi}} \quad (\text{B.6})$$

$$v_I = - \frac{4R}{\pi E} \int_0^1 g(\tau) * \log \left| \frac{1 + \sqrt{\tau(s)}}{1 - \sqrt{\tau(s)}} \right| d\tau \quad (\text{B.7})$$

No special distribution of $g(s)$ is presumed in Equations B.4 - B.5. For simplicity, however, the step distribution shown in Figure B.1 is assumed in the present analysis: From the crack tip to $s = s_0$ we have $g(s) \equiv \sigma_T$ and from $s = s_0$ to the crack front we have $g(s) \equiv \sigma_F$. It is assumed that both $|\sigma_T|$ and $|\sigma_F|$ are less than or equal to σ_1 .

REFERENCE STATE: MAXIMUM LOAD

The reference state is defined by $\sigma = \sigma_{\text{MAX}}$ and $\sigma_T = \sigma_F = \sigma_1$. The stress intensity factor is expressed by

$$K_{\text{MAX}} = \sigma_{\text{MAX}} \sqrt{\pi l} \quad (\text{B.8})$$

Equations B.4 - B.7 give us the following well-known expressions for the reference crack front shape,

$$\frac{R_0}{l} = \frac{\pi}{8} \left(\frac{\sigma_{\text{MAX}}}{\sigma_1} \right)^2 \quad (\text{B.9})$$

$$\frac{\delta_{\text{MAX}}}{l} = \frac{\pi}{E} \frac{\sigma_{\text{MAX}}^2}{\sigma_1} \quad (\text{B.10})$$

The reference crack opening in general can be described by

$$\frac{v_0}{\delta_{\max}} = f(s) \quad (\text{B.11})$$

where $f(s) \equiv 0$ at $s < 0$ and

$$f(s) = \sqrt{s} - \frac{1}{4}(1-s)\log_{\epsilon}\left(\frac{1+\sqrt{s}}{1-\sqrt{s}}\right)^2; (s \geq 0) \quad (\text{B.12a})$$

for which the following features exist (3,4)

$$f(s) = 2\sqrt{s} - s*f(1/s) \quad (\text{B.12b})$$

$$\approx \begin{cases} s^2 & \text{at } s \leq 1 \\ 2\sqrt{s} - 1/s & \text{at } s > 1 \end{cases} \quad (\text{B.12c})$$

CLOSURE STATE: MINIMUM LOAD

The following crack opening expressions are obtained solving Equations B.4 - B.7 with the simple coherent stress distribution shown in Figure B.1,

$$\frac{v}{\delta_{\max}} = \frac{\sigma_F}{\sigma_1} * f(s) + \sqrt{s_0} \left(p - \frac{\sigma_F}{\sigma_1}\right) * f\left(\frac{s}{s_0}\right) \quad (\text{B.13a})$$

$$\begin{aligned} & \left[\frac{\sigma_F}{\sigma_1} + p - \frac{(p - \sigma_F/\sigma_1)}{s_0^{3/2}} \right] * s^2 \\ \frac{v}{\delta_{\max}} \approx & \begin{cases} \frac{\sigma_F}{\sigma_1} s^2 + (p - \frac{\sigma_F}{\sigma_1})(2\sqrt{s} - \frac{s_0^{3/2}}{s}) & (\text{B.13b}) \\ \frac{\sigma_F}{\sigma_1}(2\sqrt{s} - \frac{1}{s}) + (p - \frac{\sigma_F}{\sigma_1})(2\sqrt{s} - \frac{s_0^{3/2}}{s}) \end{cases} \end{aligned}$$

The approximate expressions apply at $s \leq s_0$, $s_0 < s \leq 1$ and $1 < s$ respectively.

Equations B.13 apply, of course, only as long as non-negative values are predicted. Concentrating on the approximates Expression B.13b this means

$$\frac{\sigma_F}{\sigma_1} \leq \frac{p}{1 - \frac{s_0^{3/2}}{s}} \quad (\text{B.14})$$

which always applies when $\sigma_F/\sigma_1 \leq p$. When $\sigma_F/\sigma_1 > p$ and σ_F/σ_1 is related to s_0 as given by the equality of Expression B.14 a crack opening of $v \equiv 0$ is predicted at $s \leq s_0$.

The following relations between coherent stresses at the crack tip and crack front,

$$\frac{\sigma_F}{\sigma_1} = \frac{p - (\sigma_T/\sigma_1)\sqrt{s_0}}{1 - \sqrt{s_0}} \quad \text{or} \quad \frac{\sigma_T}{\sigma_1} = \frac{p - (1 - \sqrt{s_0})(\sigma_F/\sigma_1)}{\sqrt{s_0}} \quad (\text{B.15})$$

ensure a constant front zone width equal to the reference quantity, R_0 , expressed by Equation B.9.

It is noticed from Equations 12 that $v/\delta_{\text{MAX}} \rightarrow 2p/s$ as $s \rightarrow \infty$ irrespective of σ_F/σ_1 and s_0 . This means that the present analysis theoretically is valid only when $p \geq 0$. (No forces are considered on the crack surface at $s > 1$).

The crack front opening, δ at $s = 1$, in particular is given by

$$\frac{\delta}{\delta_{\text{MAX}}} = \frac{\sigma_F}{\sigma_1} + (p - \frac{\sigma_F}{\sigma_1})(2 - \frac{f(s_0)}{\sqrt{s_0}}) \quad (\text{B.16a})$$

$$\approx \frac{\sigma_F}{\sigma_1} + (p - \frac{\sigma_F}{\sigma_1})(2 - s_0^{3/2}) \quad (\text{B.16b})$$

The opening at $s = s_0$ where the stress of coherence changes discontinuously is given by

$$\frac{v(s_0)}{\delta_{\text{MAX}}} = \frac{\sigma_F}{\sigma_1} f(s_0) + (p - \frac{\sigma_F}{\sigma_1})\sqrt{s_0} \quad (\text{B.17b})$$

$$\approx \frac{\sigma_F}{\sigma_1} s_0^2 + (p - \frac{\sigma_F}{\sigma_1})\sqrt{s_0} \quad (\text{B.17b})$$

Reference crack closure state: $\sigma_F = -1$

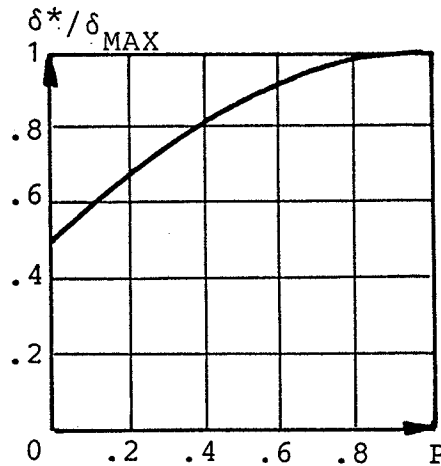


Figure B.2. Reference crack closure front opening, δ^* .

Of special interest is the location, $s_0 = s_0^*$, below which the crack opening remains a constant during load

reduction with a maximum compressive coherent stress of $\sigma_F = -\sigma_1$. We get from Equation B.13b

$$s_0^* \approx \left(\frac{1+p}{2} \right)^{2/3} \quad (\text{B.18})$$

giving

$$\frac{v^*}{\delta_{\max}} \approx \begin{cases} s^2 & ; (0 \leq s \leq s_0^*) \\ (1+p)(2\sqrt{s} - \frac{1+p}{2s}) - s^2 & ; (s_0^* \leq s \leq 1) \end{cases} \quad (\text{B.19})$$

The crack front opening

$$\frac{\delta^*}{\delta_{\max}} \approx \frac{1}{2} (1 + 2p - p^2) \quad (\text{B.20})$$

is shown graphically in Figure B.2.

The coherent stress, σ_T^* , is obtained from Equation B.15 with $s_0 = s_0^*$ from Equation B.18. We get

$$\frac{\sigma_T^*}{\sigma_1} = 2 \left(\frac{1+p}{2} \right)^{2/3} - 1 \quad (\text{B.21})$$

Relaxation states:

$$p\sigma_1 > \sigma_F > -\sigma_1;$$

From the reference closure state the coherent stresses will start relaxing. This means that σ_F will increase from $\sigma_F = -\sigma_1$. It is noticed from Equation B.14 that any s_0 is permissible as long as $\sigma_F/\sigma_1 \leq p$.

The following Equations apply especially for $s_0 \equiv s_0^*$ as expressed by Equation B.18.

$$\frac{v}{\delta_{\max}} \approx \begin{cases} \left[\frac{\sigma_F}{\sigma_1} + 2 \frac{p - \frac{\sigma_F}{\sigma_1}}{1+p} \right] s^2 & ; (0 \leq s \leq s_0^*) \\ \frac{\sigma_F}{\sigma_1} s^2 + \left(p - \frac{\sigma_F}{\sigma_1} \right) \left(2\sqrt{s} - \frac{1+p}{2s} \right) & ; (s_0^* \leq s \leq 1) \end{cases} \quad (\text{B.22})$$

with

$$\frac{\delta}{\delta_{\max}} \approx \frac{1}{2} [p(3-p) - (1-p) \frac{\sigma_F}{\sigma_1}] \quad (\text{B.23})$$

The coherent stress, σ_T , is given by Equation B.15 with $s_0 = s_0^*$.

The special choice of s_0 applied above means that the zone of compressive coherent stresses is considered

constant. At least for the introductory relaxation state this statement is plausible.

$$\sigma_F = p\sigma_1:$$

At $\sigma_F = p\sigma_1$, Equation B.13b reduces as follows

$$\frac{v}{\delta_{\max}} \approx p s^2 \quad (\text{B.24})$$

with $\delta = p\delta_{\max}$. Equation B.15 predicts the coherent stresses to be uniformly distributed with

$$\frac{\sigma_T}{\sigma_1} = \frac{\sigma_F}{\sigma_1} = p \quad (\text{B.25})$$

$$\sigma_F > p\sigma_1:$$

As indicated previously some restrictions apply on σ_F in this area. The locations, $s \leq s_0$ at which $v \equiv 0$ is given by Equation B.14. We get

$$s_0 \approx \left(1 - \frac{P}{\sigma_F/\sigma_1}\right)^{2/3} \quad (\text{B.26})$$

which produces

$$\frac{v}{\delta_{\max}} \approx \begin{cases} 0 & ; (s \leq s_0) \\ \frac{\sigma_F}{\sigma_1} s^2 + \left(p - \frac{\sigma_F}{\sigma_1}\right) \left(2\sqrt{s} + \frac{P - (\sigma_F/\sigma_1)}{s(\sigma_F/\sigma_1)}\right) & ; (s_0 < s \leq 1) \end{cases} \quad (\text{B.27})$$

with

$$\frac{\delta}{\delta_{\max}} \approx \frac{\sigma_F}{\sigma_1} - \left(\frac{\sigma_F}{\sigma_1} - p\right) \left(1 + \frac{P}{\sigma_F/\sigma_1}\right) \quad (\text{B.28})$$

at a coherent stress, σ_T , of

$$\frac{\sigma_T}{\sigma_1} = \frac{\sigma_F}{\sigma_1} \left[1 - \left(1 - \frac{P}{\sigma_F/\sigma_1}\right)^{2/3}\right] \quad (\text{B.29})$$

At s_0 greater than expressed by Equation B.26 positive crack openings are predicted by Equation B.13b for any s .

For $\sigma_F > p\sigma_1$ it is plausible to think of a relaxation mechanism which acts mainly by expansion of a zone of maximum tensile coherent stress, $\sigma_F = \sigma_1$. The expansion will start, corresponding to $s_0 = 1$, and end as given

by Equation B.26 with $\sigma_F/\sigma_1 = 1$. For the special case of $\sigma_F = \sigma_1$ we get from Equations B.13b and B.15

$$\frac{V}{\delta_{MAX}} \approx \left(\frac{1 - \frac{1-p}{s_0^{3/2}}}{s^2 - (1-p)(2\sqrt{s} - \frac{s_0^{3/2}}{s})} \right) * s^2 \quad (B.30)$$

with

$$\frac{\delta}{\delta_{MAX}} \approx 1 - (1-p)(2 - s_0^{3/2}) \quad (B.31)$$

$$\frac{\sigma_T}{\sigma_F} = 1 - \frac{1-p}{\sqrt{s_0}} \quad (B.32)$$

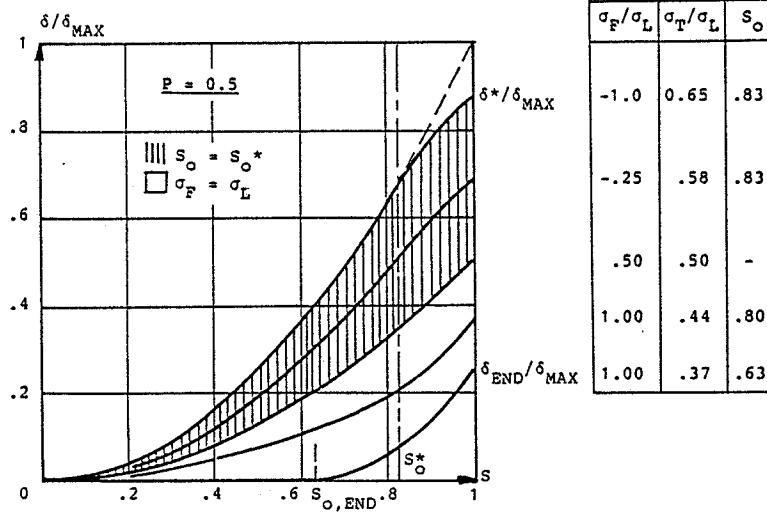


Figure B.3. Shape of crack front as related to coherent stress relaxation after crack closure with $p = 0.5$.

End state:

The end state of relaxation is defined by $\sigma_F = \sigma_1$ and

$$s_0 = s_{0,END} \approx (1-p)^{2/3} \quad (B.33)$$

From the preceding section we get

$$\frac{V_{END}}{\delta_{MAX}} \approx \begin{cases} 0 & ; (s \leq s_0) \\ s^2 - (1-p)(2\sqrt{s} - \frac{1-p}{s}) & ; (s_0 < s \leq 1) \end{cases} \quad (B.34)$$

with

$$\frac{\delta_{END}}{\delta_{MAX}} \approx p^2 \quad (B.35)$$

at a coherent stress of

$$\frac{\sigma_{T,END}}{\sigma_1} \approx 1 - (1 - p)^{2/3} \quad (B.36)$$

It is noticed from comparing Equations B.18 and B.33 that $s_{0,END} < s_0^*$ and $s_{0,END} > s_0^*$ at $p > 1/3$ and $p < 1/3$ respectively. At $p = 1/3$ we have $s_{0,END} = s_0^*$.

DEDUCTIONS

Two states of relaxation are identified in the preceding section. They are demonstrated in Figure B.3 considering a load ratio of $p = 0.5$:

State 1: For $\sigma_F < p\sigma_1$ the elastic crack front shapes are approximately congruent - meaning that the whole crack front in this area can be given a time history such that a "frozen" viscoelastic shape can be predicted by Equation B.3. (A closing viscoelastic "opening" trend is not possible as this would implicate negative yield in $s < s_0$).

State 2: At $\sigma_F > p\sigma_1$ the elastic openings for $s < s_{0,END}$ can still be considered practically congruent. For $s > s_{0,END}$, however, they can not. This means that the latter area in the viscoelastic crack will now start opening. A tensile flow zone (σ_1) will spread from $s = 1$ towards $s = s_{0,END}$. At this stage no crack closure effects are left to reduce crack opening of the viscoelastic crack.

In other words: A lower bound on relaxation is approached at the crack front which is comparable with crack opening under minimum load. We summarize,

$$\sigma = \sigma_{MIN} \quad (B.37)$$

$$R_{END} = (1 - s_{0,END}) * R_0 = [1 - (1 - p)^{2/3}] * R_0 \quad (B.38)$$

$$\delta_{END} = p^2 \delta_{MAX} \quad (B.39)$$

AVERAGING

Two crack front widths are relevant when considering crack propagation in materials subjected to square wave loading: The reference width, R_0 , applying at σ_{\max} as expressed by Equation B.9 - and the smaller width, R_{END} , given by Equation B.38 applying at the end of total relaxation.

R_0 and R_{END} become relevant at long times at maximum load and minimum load respectively. However, in order to simplify calculations the maximum front width, R_0 , will always be the one referred to.

This means that the relaxation end state previously considered has to be appropriately modified: We introduce a fictitious end opening,

$$V_{\text{END, FICT}} = H * \delta_{\max} * S^2 \quad (\text{B.40})$$

referring to R_0 which produce the same rate of crack propagation as the real end state would predict. The parameter, H , is determined in the following way:

A viscoelastic material like wood is considered with Power Law creep, $C(t) = 1 + (t/\tau)^{1/4}$ where t , C , and τ mean time, normalized creep function, and relaxation time respectively.

From (5) may be derived that a crack (with coherent stress $\equiv \sigma_1$) extends its length by a distance equal to the immediate front zone width (R) in a period of time, Ω , determined by

$$\Omega = 3 * \tau (\delta_{\text{cr}} / \delta - 1)^4 \quad (\text{B.41})$$

where

$$\frac{\delta}{\delta_{\text{cr}}} = k * SL^2 \quad (\text{B.42})$$

As usual load level is denoted by $SL = \sigma / \sigma_{\text{cr}}$ where σ is load and σ_{cr} is strength. The damage ratio is $k = l/l_0$ = crack length considered/initial crack length. The so-called critical crack opening displacement (COD) is denoted by δ_{cr} .

Considering now the real end state situation

$$\Omega_{\text{END}} = 3\tau * \left(\frac{\delta_{\text{cr}}}{p^2 \delta_{\max}} - 1 \right)^4 \quad (\text{B.43})$$

involving a rate of propagation

$$\frac{dk}{dt} = \frac{R_{END}}{\Omega_{END}} = \frac{1 - s_{0,END}}{3\tau} \left(\frac{\delta_{END}}{p^2 \delta_{MAX}} - 1 \right)^{-4} \quad (B.44)$$

In a similar way we get

$$\frac{dk}{dt} = \frac{R_0}{\Omega_0} = \frac{1}{3\tau} \left(\frac{\delta_{END}}{H^* \delta_{MAX}} - 1 \right)^{-4} \quad (B.45)$$

considering the fictitious end state.

Equations B.44, B.45, and B.42 together with B.33 produce

$$H = \frac{p^2 [1 - (1-p)^{2/3}]^{1/4}}{1 - p^2 kSL_{MAX}^2 [1 - [1 - (1-p)^{2/3}]^{1/4}]} \quad (B.46a)$$

or

$$H \approx \frac{p^{2.5}}{1 - p^2 (1-\sqrt{p}) kSL_{MAX}^2} \approx p^{2.5} \quad (B.46b)$$

where the latter approximation applies because $0 \leq kSL_{MAX}^2 \leq 1$ and $0 \leq p \leq 1$.

It should be emphasized that the introduction of a fictitious end state is only a "trick" to facilitate life-time calculations of square wave loaded materials by always referring to the maximum crack front width, R_0 . With a constant coherent stress of size σ_1 the fictitious end state is not a state at equilibrium.

Practically the considerations above are used in the main text of the article to simplify calculations by stating the following approximation: A closed viscoelastic crack starts opening when the associated elastic crack front opening, δ , has relaxed to $H^* \delta_{MAX}$.

Considering the approximate nature of the problem it is easily checked by Equation B.20 that we may as well state that the opening process just mentioned starts when the associated elastic crack front opening, δ , has relaxed to $H^* \delta^*$ where δ^* is the reference crack closure front opening shown in Figure B.2.

It has been indicated in the introductory to this appendix that the results here obtained are subjected to some modifications (a.o. considering crack surface contact at $s > 1$) when used to predict lifetime of real materials.

The parameter, H , however, is anticipated to apply without modification because it represents total relaxation.

LITERATURE - APPENDIX B

- 1) Rice, J. R.: "Mechanics of Crack-Tip Deformation and Extension by Fatigue". Fatigue Crack Propagation, ASTM STP 415(1967), 247-311.
- 2) Barenblatt, G. I.: "The mathematical Theory of Equilibrium Cracks in brittle Fracture". Advances in Appl. Mech., 7(1962), 55-129.
- 3) Nielsen, L. Fuglsang: "Fatigue of Elastic Materials" (in danish). Techn. Univ. Denmark, Build. Mat. Lab., progress report, november 1984, on project, StvF 16-3179.B972.
- 4) Nielsen, L. Fuglsang: "Fatigue of Viscoelastic Materials - especially Wood" (in danish). Techn. Univ. Denmark, Build. Mat. Lab., progress report, feb. 1985, on project, StvF 16-3179.B972.
- 5) Nielsen, L. Fuglsang: "A Lifetime Analysis of Cracked Linear Viscoelastic Materials - with Special Reference to Wood". IUFRO-Engineering Group Meeting, Borås, Sweden 1982. Proc. IUFRO S5.02, Chalmers Univ. of Technology, Dept. Civil Eng., Gothenburg 1982, 151-178. (previously available as Techn. Rep. 92/80, Build. Mat. Lab., Techn. Univ. of Denmark, Copenhagen, 1980.

APPENDIX C

NUMERICAL LIFETIME ANALYSIS

This section outlines a numerical lifetime analysis based on the theory given in the main text of the article.

Equations previously developed in the article are "sorted" and presented in a way which is appropriate for computer calculation.

A FORTRAN program following the principles of the "flow" presented below is given in the subsequent section.

NUMERICAL METHOD

For the purpose of calculating damage rate we rewrite Equation 4.35 as follows

$$Y = A*X^b + B*X - D = 0 \quad (C.1)$$

where the inverse damage rate is denoted by

$$X = dt/dk \quad (C.2)$$

The parameters, A, B and D, have been evaluated observing the generalization procedure considered in Section 5.

An equation, $Y = Y(X) = 0$, can be solved using the Newton iteration method,

$$X_{NEW} = X_{OLD} - \frac{Y(X_{OLD})}{(dY/dX)_{X,OLD}} \quad (C.6)$$

where X_{OLD} is an estimate. In the present context,

$$X_{NEW} = X_{OLD} - \frac{A*X_{OLD}^b + B*X_{OLD} - D}{bAX_{OLD}^{b-1} + B} \quad (C.7)$$

from which $X = dt/dk$ is determined by iteration.

Subsequently damage as a function of time, $k = k(t)$, is given by summation - and residual strength, $\sigma_{er}(t)$, as described in Section 5.

GIVEN:Material:

b	Creep power
τ	Relaxation time
FL	Strength level
f_{σ}	Interaction factor
U_{-}	Lower efficient coefficient

Load:

SL_{max}	Maximum load level
p	Load ratio
f	Load frequency
β	Relative time under maximum load

Empirical constants:

M	Damage rate power
C	Damage rate constant

DERIVED CONSTANTS:Wave period:

$$T = 1/f$$

Shift factors:

$$q = [(1+b)(2+b)/2]^{1/b}$$

$$h = [1 - n*(1 - \beta)^b]^{-1/b}$$

with

$$n = \frac{1}{2}(1 - H + n_1 - \sqrt{(1 - H - n_1)^2})$$

$$n_1 = \frac{1 - \beta^b}{(\tau/T)^b + (1 - \beta)^b}$$

$$H \approx [p + \frac{\sqrt{p^2}}{2}]^{2/b}$$

Amplification factor:

$$G = 1 + \frac{\beta^b(1-\beta)^2 - \beta^2(1-\beta)^b}{1 - 2\beta} \left(\frac{T}{\tau}\right)^b$$

$$\rightarrow 1 + \frac{2-b}{2} \left(\frac{T}{2\tau}\right)^b \quad (\text{as } \beta \rightarrow 0.5)$$

Efficiency factor:

$$U = \frac{1}{2}[1 + p + (\sqrt{p^2} - p)U_{-}]$$

Critical damage ratio:

$$k_{cr} = \frac{2f_0^2}{SL_{max}^2} [1 + \sqrt{1 + 4 f_0^2 (f_0^2 - 1) / SL_{max}^4}]^{-1}$$

Damage increment for summation:

$$\Delta k = k_{cr} / 1000 \text{ (for example)}$$

Effective strength level:

$$FL \Rightarrow f_0 FL$$

CALCULATION

t (= 0 at start)

k (=1 at start)

X = dt/dk (estimate X = 10 f.ex. at start)

LABEL 1

$$f_1 = [f_0^2 - (f_0^2 - 1)k^2]^{-1/2}$$

$$SL_{max} \Rightarrow f_1 SL_{max}$$

$$p_{eff} = 1 - [(1-p)U]^{M/4} [SL_{max}/k]^{(M/4-1)}$$

$$A = [1 - \frac{C^b(1-p_{eff})^{2+b}(1-8h^b)}{2^{1+2b}}] * (\frac{\pi^2 FL^2}{8qh\tau} - k SL_{max}^2)^b$$

$$B = \frac{\pi^2 C * G * FL^2}{64T} - (1-p_{eff})^4 k SL_{max}^2$$

$$D = \frac{1 - k * SL_{max}^2}{k * SL_{max}^2}$$

Calculate X = dt/dk:

$$X_{old} = X$$

LABEL 2

$$X_{new} = X_{old} - \frac{A * X_{old}^b + B * X_{old} - D}{b * X_{old}^{b-1} + B}$$

if(abs(1-X_{old}/X_{new}).gt.0.001) goto LABEL 3

if(X_{new}.gt.0) X = X_{new}

if(X_{new}.le.0) X = X_{old}/2

goto LABEL 2

LABEL 3

$$N = t/T$$

$$\frac{\sigma_{cr}(N)}{\sigma_{cr}} = [\frac{f_0^2 - (f_0^2 - 1)k^2}{k}]^{1/2}$$

WRITE k, t, N, $\sigma_{cr}(N)/\sigma_{cr}$

Calculate time, t, and damage ratio, k:

```

Nt = X*Nk
t = t + Nt
k = k + Nk
if(kk.gt.kcr) goto LABEL 4
goto LABEL 1

LABEL 4

END

```

FORTRAN PROGRAM

The FORTRAN program presented below follows in principles the outlines given in the preceding section.

Output data are: Fatigue-life (time and load cycles to failure), relative residual strength, and relative critical stress intensity factor as a function of progressing fatigue.

The program also calculates dead-load lifetime, t_{dead} , at $SL \equiv SL_{MAX}$ (and corresponding residual strength) which is of interest when evaluating the lower frequency results of the fatigue analysis. The expressions needed for this purpose are given in Section 6.1.

PROGRAM

```

C*****
C* PROGRAM NAME: VIS-FAT.FOR (Viscoelastic Fatigue) *
C*****
C* LIFETIME OF SQUARE-WAVE LOADED, MULTI-DAMAGED VISCOELASTIC MATERIALS *
C* AS A FUNCTION OF: 1) MAX LOAD, 2) MIN/MAX LOAD, 3) FREQUENCY, AND 4) *
C* RELATIVE TIME UNDER MAX LOAD - RELATIVE REDUCTIONS OF STRENGTH AND *
C* CRITICAL STRESS INTENSITY FACTOR (LONG CRACKS) ARE INCLUDED AS FUNC- *
C* TIONS OF PROGRESSIVE FATIGUE - ALSO INCLUDED IS DEADLOAD LIFETIME *
C* AT LOAD CONSTANTLY AT MAXIMUM (July 13, 1987, L. Fugleang Nielsen) *
C*****
C
      implicit real (a-h,k-z),integer(i-j)
      integer out
      dimension ff(13),ssimax(7)
C INPUT DATA *****
C Meaning of symbols: See Format 200 *****
      data b/0.25/,tau/1.000/,f1/0.15/,f0/1.500/,umin/0.40/,
      sp/0.000/,beta/0.50/,
      sm/9.00/,c/3.00/,
      tincrkh/500/,incrcut/30/
      pi=3.14159
      ssimax(1)=0.55
      ssimax(2)=0.6

```

```

      sblmax(3)=0.7
      sblmax(4)=0.8
      sblmax(5)=0.85
      sblmax(6)=0.9
      sblmax(7)=0.95
      ff(1)=1.e-10
      ff(2)=1.e-8
      ff(3)=1.e-6
      ff(4)=1.e-4
      ff(5)=1.e-2
      ff(6)=1.e-1
      ff(7)=1.
      ff(8)=1.e+1
      ff(9)=1.e+2
      ff(10)=1.e+4
      ff(11)=1.e+6
      ff(12)=1.e+8
      ff(13)=1.e+10
C DERIVED CONSTANTS *****
      fl=ff-f0*fl
C *****
      q=((1.+b)*(2.+b)/2.)*(1./b)
C *****
      u=0.5*(1.+p*(abs(p)-p)*umin)
C *****
C SELECT LOAD, BLmax. Calculate critical damage ratio *****
      do 6 i=1,1
      sblmax=sblmax(i)
      kcr=2.*f0**2./sblmax**2./(1.+sqrt(1.+4.*f0**2.*(f0**2.-1.)
      */sblmax**4.))
C *****
C INCREMENTS *****
      dk=(kcr-1.)/float(incr)
      out=incr/incrout
C DEADLOAD LIFETIME AT SL = BLmax *****
      cc=8.*q*tau/pi**2./fl**2.
      t=0.
      k=1.
      5 fl=1./sqrt(f0**2.-(f0**2.-1.)*k**2.)
      sblmaxff=f1*sblmax
      skk=k*sblmaxff**2.
      ddt=cc*dk*(1./skk-1.)*(1./b)/skk
      t=t+ddt
      k=k+dk
      if(k.ge.kcr) goto 7
      goto 5
      7 tdead=t
C MAIN TEXT *****
      write(1,200) b,tau,f1,f0,sblmax,p,beta,m,c,incr,incrout,tdead
200 format('1',5x,//////////
      $      6x,'FATIGUE OF MULTI-DAMAGED VISCOELASTIC MATERIALS'/
      $      6x,'*****',
      $'****'/
      $      6x,'b = ',f4.2,'      (creep power)'/
      $      6x,'TAU = ',f4.1,' days (relaxation time)'/
      $      6x,'PL = ',f4.2,'      (strength level)'/
      $      6x,'f0 = ',f4.2,'      (interact. factor)'/
      $      6x,'BLMAX = ',f4.2,'    (load level)'/
      $      6x,'P = ',f4.2,'      (load ratio)'/
      $      6x,'BETA = ',f4.2,'    (rel. time under max load)'/
      $      6x,'m = ',f4.2,'      (damage rate power)'/
      $      6x,'c = ',f4.2,'      (damage rate constant)'/
      $      6x,'incr = ',i6,'      (size of partitions: (Kcr-1)/incr)'/
      $      6x,'incrout = ',i3,'   (appr. numb. of outputs)'/
      $      6x,'DEADLOAD lifetime at SL = BLmax: Tdead = ',1p10.3,
      $      ' days'/
      $      6x,'*****',
      $'****',/
      $'1')
C *** SELECT FREQUENCY *****
C START CALCULATE *****
      do 6 i=7,7

```

```

f=ff(ii)
tp=(1./f)/(24.*3600.)
C *** frequency dependent "CONSTANTS", g and h *****
gg=beta**b*(1.-beta)**2.-beta**2.*(1.-beta)**b
ggg=1.-2.*beta
gggg=(tp/tau)**b
if(ggg.ne.0.) q=1.+gg*gggg/qqq
if(ggg.eq.0.) q=1.+0.5*((2.-b)*(tp/tau/2.))**b)
C *****
d1=(1.-beta**b)/((tau/tp)**b+(1.-beta)**b)
hh=((p+abs(p))/2.))**2.5
delta=0.5*(1.-hh+d1-sqrt((1.-hh-d1)**2.))
h=(1.-delta*(1.-beta)**b)**(-1./b)
C *****
write(*,300) f, tp
300 format('0',5x,'LOAD CYCLE: f = ',1p10.3,' Hz(cycles/sec)'/
'      5x,'= 1 cycle per ',1p10.3,' days'//
'      5x,'TIME(days)',5x,' LOG(N) ',5x,'DAMAGE ',
'      5x,' STRENGTH',5x,' Kcr'//)
C CALCULATE (init. x = dt/dk = 10 is arbitrary guess) *****
t=0.
cycles=t/tp+1.e-10
logn=log10(cycles)
k=1.
f1=1./sqrt(f0**2.-(f0**2.-1.)*k**2.)
strength=1./(f1*sqrt(k))
kcrit=1./f1
x=10.
i=0
1 f1=1./sqrt(f0**2.-(f0**2.-1.)*k**2.)
slmaxeff=f1*slmax
sk=slmaxeff*sqrt(k)
pfff=1.-((1.-p)*u)**(m/4.)*k**2.(m/4.-1.)
aa=c**b*(1.-pfff)**(2.+b)*(1.-beta**b)
aaa=2.*(1.+2.*b)
aaaa=(pi*f1*sk**2.)/(5.*q*tau)**b
a=(1.-aa/aaa)*aaaa
bb=pi**2.*c*q*f1*sk**2.*(1.-pfff)**4.*k**2./(64.*tp)
d=(1.-sk**2.)/sk**2.
C *** x = dt/dk *****
xold=x
2 xnew=xold-(a*xold**b+bb*xold-d)/(b*a*xold**(b-1.))+bb)
if(abs(1.-xold/xnew).le.0.001) goto 3
if(xnew.le.0.) xold=xold/2.
if(xnew.gt.0.) xold=xnew
goto 2
3 if(i.eq.0) goto 5
if(k+dk.ge.kcr) goto 5
if(i.ne.out) goto 4
5 write(*,100) t,logn,k,strength,kcrit
100 format('0',5x,1p10.3)
if(k+dk.ge.kcr) goto 11
i=0
4 i=i+1
x=xnew
C *** TIME, t, CYCLES, N, AND DAMAGE RATIO, k *****
dt=x*dk
t=t+dt
cycles=t/tp
logn=log10(cycles)
k=k+dk
C *** RESIDUAL STRENGTH AND CRITICAL STRESS INTENSITY FACTOR *****
strength=1./(f1*sqrt(k))
C *** Kcr(k)/Kcr(1)=1/f1 *****
kcrit=1./f1
goto 1
11 ndead=tdead/tp
lgndead=log10(ndead)
write(*,700) lgndead
700 format('0',5x,'DEADLOAD: ("Ndead"=f*Tdead), log("Ndead") = ',
1p10.3//)
6 continue

```

```
stop
end
```

EXAMPLE (FIGURE 6.5)

FATIGUE OF MULTI-DAMAGED VISCOELASTIC MATERIALS

```
*****
```

```
b = .25      (creep power)
TAU = 1.0 days (relaxation time)
FL = .15     (strength level)
f0 = 1.50    (interact. factor)
SLMAX = .55  (load level)
P = .00      (load ratio)
BETA = .50   (rel. time under max load)
n = 7.00     (damage rate power)
c = 3.00     (damage rate constant)
```

```
incrk = 500 (size of partitions: (Kcr-1)/incrk)
incrcut = 30 (appr. numb. of outputs)
```

```
DEADLOAD lifetime at SL = SLmax: Tdead = 2.156E+02 days
*****
```

```
LOAD CYCLE: f = 1.000E+00 Hz (cycles/sec)
= 1 cycle per 1.157E-05 days
```

TIME(days)	LOG(N)	DAMAGE	STRENGTH	Kcr
.000E+00	-1.000E+01	1.000E+00	1.000E+00	1.000E+00
1.855E-01	4.205E+00	1.007E+00	9.879E-01	9.915E-01
3.483E-01	4.478E+00	1.014E+00	9.752E-01	9.822E-01
4.966E-01	4.627E+00	1.022E+00	9.624E-01	9.728E-01
6.147E-01	4.723E+00	1.029E+00	9.496E-01	9.632E-01
7.226E-01	4.775E+00	1.036E+00	9.367E-01	9.535E-01
8.160E-01	4.848E+00	1.043E+00	9.237E-01	9.436E-01
8.966E-01	4.889E+00	1.051E+00	9.107E-01	9.335E-01
9.659E-01	4.921E+00	1.058E+00	8.976E-01	9.232E-01
1.025E+00	4.947E+00	1.065E+00	8.844E-01	9.128E-01
1.076E+00	4.968E+00	1.072E+00	8.711E-01	9.021E-01
1.119E+00	4.985E+00	1.080E+00	8.578E-01	8.913E-01
1.155E+00	4.999E+00	1.087E+00	8.443E-01	8.802E-01
1.185E+00	5.010E+00	1.094E+00	8.308E-01	8.689E-01
1.210E+00	5.019E+00	1.101E+00	8.171E-01	8.574E-01
1.231E+00	5.027E+00	1.107E+00	8.033E-01	8.457E-01
1.248E+00	5.033E+00	1.116E+00	7.893E-01	8.337E-01
1.262E+00	5.038E+00	1.123E+00	7.752E-01	8.215E-01
1.273E+00	5.041E+00	1.130E+00	7.610E-01	8.090E-01
1.282E+00	5.044E+00	1.137E+00	7.466E-01	7.963E-01
1.289E+00	5.047E+00	1.145E+00	7.320E-01	7.832E-01
1.295E+00	5.049E+00	1.152E+00	7.173E-01	7.698E-01
1.299E+00	5.050E+00	1.159E+00	7.023E-01	7.561E-01
1.302E+00	5.051E+00	1.166E+00	6.871E-01	7.421E-01
1.304E+00	5.052E+00	1.174E+00	6.717E-01	7.277E-01
1.306E+00	5.052E+00	1.181E+00	6.561E-01	7.129E-01
1.307E+00	5.053E+00	1.188E+00	6.401E-01	6.978E-01
1.307E+00	5.053E+00	1.195E+00	6.239E-01	6.821E-01
1.308E+00	5.053E+00	1.203E+00	6.074E-01	6.661E-01
1.308E+00	5.053E+00	1.210E+00	5.905E-01	6.495E-01
1.308E+00	5.053E+00	1.217E+00	5.732E-01	6.324E-01
1.308E+00	5.053E+00	1.224E+00	5.555E-01	6.147E-01
1.308E+00	5.053E+00	1.226E+00	5.510E-01	6.102E-01

```
DEADLOAD: ("Ndead"=f*STdead), log("Ndead") = 7.270E+00
```

Stop - Program terminated.

SHORT VERSION PROGRAM

```

C This program is a short version, VIS-FAT1.FOR, of a more general fati-
C que program described below. Outputs are: Time and load cycles at fai-
C lure (and deadload lifetime at constant max load).      (July 14, 1987)
C *****
C* PROGRAM NAME: VIS-FAT.FOR (Viscoelastic Fatigue)      *
C *****
C* LIFETIME OF SQUARE-WAVE LOADED, MULTI-DAMAGED VISCOELASTIC MATERIALS *
C* AS A FUNCTION OF: 1) MAX LOAD, 2) MIN/MAX LOAD, 3) FREQUENCY, AND 4) *
C* RELATIVE TIME UNDER MAX LOAD - STRENGTH REDUCTION IS INCLUDED AS A *
C* FUNCTION OF PROGRESSING FATIGUE - ALSO INCLUDED IS DEADLOAD LIFETIME *
C* AT LOAD CONSTANTLY AT MAXIMUM      (July 13, 1987, L. Fuglsang Nielsen) *
C *****

```

```

C
      implicit real (a-h,k-z),integer(i-j)
      integer out
      dimension ff(13),ss1max(8),tautau(5),ff11(3)
C INPUT DATA *****
C Meaning of symbols: see FORMAT 200 *****
      data b/0.25/,f0/1.000/,umin/0.40/,
      *p/0.000/,beta/0.50/,
      *m/9.00/,c/3.00/,
      *incrk/100/,tol/0.01/
      pi=3.14159
      ff11(1)=0.25
      ff11(2)=0.40
      ff11(3)=0.50
      do 6 ixx=1,1
      fl=ff11(ixx)
      tautau(1)=.1
      tautau(2)=.3
      tautau(3)=1.
      tautau(4)=3.
      tautau(5)=10.
      do 6 ix=3,3
      tau=tautau(ix)
      ss1max(1)=0.20
      ss1max(2)=0.30
      ss1max(3)=0.40
      ss1max(4)=0.50
      ss1max(5)=0.60
      ss1max(6)=0.70
      ss1max(7)=0.80
      ss1max(8)=0.90
      ff(1)=1.e-10
      ff(2)=1.e-6
      ff(3)=1.e-4
      ff(4)=1.e-2
      ff(5)=1.e-1
      ff(6)=1.
      ff(7)=1.e+1
      ff(8)=1.e+2
      ff(9)=1.e+4
      ff(10)=1.e+6
      ff(11)=1.e+10
C DERIVED CONSTANTS *****
      fl=ff*f0*fl
C *****
      q=((1.+b)*(2.+b)/2.)*(1./b)
C *****
      u=0.5*(1.+p+(abs(p)-p)*umin)
C *****
C MAIN TEXT *****

```

```

      write(1,200) b,tau,f1,f0,p,beta,m,c,incr,k,tol
200 format('1',5x,/)
      $      $x,'FATIGUE OF MULTI-DAMAGED VISCOELASTIC MATERIALS'//
      $      $x,'*****'//
      $      $x,'b = ',f4.2,'      (creep power)'//
      $      $x,'TAU = ',f7.2,'      days (relaxation time)'//
      $      $x,'FL = ',f4.2,$x,' (strength level)'//
      $      $x,'f0 = ',f4.2,$x,' (interact. factor)'//
      $      $x,'P = ',f5.2,'      (load ratio)'//
      $      $x,'BETA = ',f4.2,'      (rel. time under max load)'//
      $      $x,'m = ',f5.2,'      (damage rate power)'//
      $      $x,'c = ',f5.2,'      (damage rate constant)'//
      $      $x,'incr = ',f6.2,' (= step(k)/(Kcr-1) in analysis)'//
      $      $x,'tol = ',f5.3,'      (tolerance on time increments)'//
      $      $x,'*****'//
      $      $x,'*****'//

C SELECT LOAD, SLmax. Calculate critical damage ratio *****
      do 6 i=1,8
      slmax=slmax(i)
      kcr=2.*f0**2./slmax**2./(1.+sqrt(1.+4.*f0**2.*(f0**2.-1.)
      /slmax**4.))

C *****
C INCREMENTS *****
      dk=(kcr-1.)/float(incr)

C DEADLOAD LIFETIME AT SL = SLmax *****
      cc=8.*q*tau/pi**2./f1eff**2.
      t=0.
      k=1.
      8 f1=1./sqrt(f0**2.-(f0**2.-1.)*k**2.)
      slmaxeff=f1*slmax
      skk=k*slmaxeff**2.
      ddt=cc*dk*(1./skk-1.)*(1./b)/skk
      t=t+ddt
      k=k+dk
      if(k.ge.kcr) goto 9
      goto 8
      9 tdead=t
      write(1,800) slmax,tdead
800 format('0',/,$x,'SLMAX = ',f4.2,'      (Tdead at SL = SLMAX: ',
      $1p10.3,' days)'//
      $      $x,'*****'//
      $      $x,' FREQUENCY      PERIOD      Tcat      log(Ncat)'//
      $      $x,'      Hz      days'//)

C START CALCULATE *****
      do 6 ii=1,11
      f=ff(ii)
      tp=(1./f)/(24.*3600.)

C *** frequency dependent "CONSTANTS", g and h *****
      qq=beta**b*(1.-beta)**2.-beta**2.*(1.-beta)**b
      qgg=1.-2.*beta
      qggg=(tp/tau)**b
      if(qgg.ne.0.) q=1.+qg*qggg/qgg
      if(qgg.eq.0.) q=1.+0.5*((2.-b)*(tp/tau/2.))**b

C *****
      d1=(1.-beta**b)/((tau/tp)**b+(1.-beta)**b)
      hh=((p+abs(p))/2.)**2.5
      delta=0.5*(1.-hh+d1-sqrt((1.-hh-d1)**2.))
      h=(1.-delta*(1.-beta)**b)*(-1./b)

C *****
C CALCULATE (init. x = dt/dk = 10 is arbitrary guess) *****
      t=0.
      k=1.
      f1=1./sqrt(f0**2.-(f0**2.-1.)*k**2.)

```

```

x=10.
1 f1=1./sqrt((f0**2.-(f0**2.-1.)*k**2.)
slmax=ff=f1*slmax
sk=slmax*ff*sqrt(k)
peff=1.-((1.-p)*u)**(m/4.)*sk**(m/4.-1.)
aa=c**b*(1.-peff)**(2.+b)*(1.-beta**h**b)
aaa=2.*(1.+2.*b)
aaaa=((pi*f1*ff*sk)**2./(8.*q**h**tau))**b
a=(1.-aa/aaa)*aaaa
bb=pi**2.*c*q*f1*ff**2.*(1.-peff)**4.*sk**2./(64.*tp)
d=(1.-sk**2.)/sk**2.
C *** x = dt/dk *****
xold=x
2 xnew=xold-(a*xold**b+bb*xold-d)/(b*a*xold**(b-1.))+bb)
if(abs(1.-xold/xnew).le.tol) goto 3
if(xnew.le.0.) xold=xold/2.
if(xnew.gt.0.) xold=xnew
goto 2
3 if(k+dk.ge.kcr) goto 11
x=xnew
C *** Time, t, cycles, and damage ratio, k *****
dt=x*dk
t=t+dt
k=k+dk
goto 1
11 tcat=t
cycles=tcat/tp
logn=log10(cycles)
write(*,700) f,tp,tcat,logn
700 format(6x,4(1pE10.3,4x))
6 continue
stop
end

```

EXAMPLE OF SHORT VERSION PROGRAM RUN

```

FATIGUE OF MULTI-DAMAGED VISCOELASTIC MATERIALS
*****
b = .25      (creep power)
TAU = 1.00   days (relaxation time)
FL = .25     (strength level)
f0 = 1.00    (interact. factor)
P = .00      (load ratio)
BETA = .50   (rel. time under max load)
m = 9.00     (damage rate power)
c = 3.00     (damage rate constant)

incrk = 100  (= step(k)/(Kcr-1) in analysis)
tol = .010   (tolerance on time increments)
*****

```

```

SLMAX = .70  (Tdead at SL = SLMAX: 1.428E+01 days)
*****

```

FREQUENCY Hz	PERIOD days	Tcat days	log(Ncat)
1.000E-10	1.157E+05	2.755E+01	-3.623E+00
1.000E-06	1.157E+01	2.166E+01	2.722E-01

1.000E-04	1.157E-01	1.748E+01	2.179E+00
1.000E-02	1.157E-03	7.115E+00	3.789E+00
1.000E-01	1.157E-04	1.820E+00	4.196E+00
1.000E+00	1.157E-05	2.756E-01	4.407E+00
1.000E+01	1.157E-06	3.811E-02	4.518E+00
1.000E+02	1.157E-07	4.368E-03	4.577E+00
1.000E+04	1.157E-09	4.906E-05	4.627E+00
1.000E+06	1.157E-11	5.086E-07	4.643E+00
1.000E+10	1.157E-15	5.162E-11	4.649E+00